

Two-Piece Compaction Die Design

March 2010

Prepared by

Ethan Coffey

R&D Staff, Dynamic Systems



DOCUMENT AVAILABILITY

Reports produced after January 1, 1996, are generally available free via the U.S. Department of Energy (DOE) Information Bridge.

Web site <http://www.osti.gov/bridge>

Reports produced before January 1, 1996, may be purchased by members of the public from the following source.

National Technical Information Service
5285 Port Royal Road
Springfield, VA 22161

Telephone 703-605-6000 (1-800-553-6847)

TDD 703-487-4639

Fax 703-605-6900

E-mail info@ntis.gov

Web site <http://www.ntis.gov/support/ordernowabout.htm>

Reports are available to DOE employees, DOE contractors, Energy Technology Data Exchange (ETDE) representatives, and International Nuclear Information System (INIS) representatives from the following source.

Office of Scientific and Technical Information
P.O. Box 62
Oak Ridge, TN 37831

Telephone 865-576-8401

Fax 865-576-5728

E-mail reports@osti.gov

Web site <http://www.osti.gov/contact.html>

This report was prepared as an account of work sponsored by an agency of the United States Government. Neither the United States Government nor any agency thereof, nor any of their employees, makes any warranty, express or implied, or assumes any legal liability or responsibility for the accuracy, completeness, or usefulness of any information, apparatus, product, or process disclosed, or represents that its use would not infringe privately owned rights. Reference herein to any specific commercial product, process, or service by trade name, trademark, manufacturer, or otherwise, does not necessarily constitute or imply its endorsement, recommendation, or favoring by the United States Government or any agency thereof. The views and opinions of authors expressed herein do not necessarily state or reflect those of the United States Government or any agency thereof.

Measurement Science and Systems Engineering

TWO-PIECE COMPACTION DIE DESIGN

Ethan Coffey

Date Published: March 2010

Prepared by
OAK RIDGE NATIONAL LABORATORY
Oak Ridge, Tennessee 37831-6283
managed by
UT-BATTELLE, LLC
for the
U.S. DEPARTMENT OF ENERGY
under contract DE-AC05-00OR22725

CONTENTS

	Page
LIST OF FIGURES	v
LIST OF TABLES	ix
ABSTRACT	1
1. INTRODUCTION	1
1.1 DIE MODELS	2
1.1.1 Geometry and Materials	3
1.1.2 Model	3
1.1.3 Loading	4
2. INNER CORNER RADIUS	5
2.1 DISCUSSION	5
2.2 RESULTS	5
3. INTERFERENCE FIT	6
3.1 DISCUSSION	6
3.2 RESULTS	7
4. ADDITIONAL STUDIES	9
4.1 SMALLER WIRE DIAMETER	9
4.2 SMALLER COMPACTION FORCE	10
4.3 LARGER INNER CAVITY	10
4.4 LARGER OUTER RADIUS	11
5. REFERENCES	11
APPENDIX A. PRINCIPAL STRESS CONTOUR CHARTS	A-3

LIST OF FIGURES

Figure		Page
1	Schematic of “five-piece” powder compression die	1
2	Schematic of “two-piece” powder compression die.....	2
3	Schematic of (a) europium oxide and (b) tantalum dies	3
4	Finite-element model of europium oxide die	4
5	Finite-element model of tantalum die	4
6	Stress distribution in corner (top view).....	5
7	Stress distribution in corner (skew view).....	6
8	Maximum stress vs interference fit.....	7
9	Area of maximum wall distortion in tantalum die	8
A.1	First principal stress in europium oxide die with 0.01 in. interference fit.....	A-3
A.2	First principal stress in europium oxide die with 0.004 in. interference fit.....	A-3
A.3	First principal stress in europium oxide die with 0.003 in. interference fit.....	A-4
A.4	First principal stress in europium oxide die with 0.002 in. interference fit.....	A-4
A.5	First principal stress in europium oxide die with 0.001 in. interference fit.....	A-5
A.6	Second principal stress in europium oxide die with 0.01 in. interference fit	A-5
A.7	Second principal stress in europium oxide die with 0.004 in. interference fit	A-6
A.8	Second principal stress in europium oxide die with 0.003 in. interference fit	A-6
A.9	Second principal stress in europium oxide die with 0.002 in. interference fit	A-7
A.10	Second principal stress in europium oxide die with 0.001 in. interference fit	A-7
A.11	Third principal stress in europium oxide die with 0.01 in. interference fit.....	A-8
A.12	Third principal stress in europium oxide die with 0.004 in. interference fit	A-8
A.13	Third principal stress in europium oxide die with 0.003 in. interference fit	A-9
A.14	Third principal stress in europium oxide die with 0.002 in. interference fit	A-9
A.15	Third principal stress in europium oxide die with 0.001 in. interference fit	A-10
A.16	First principal stress in europium oxide die with 0.004 in. interference fit.....	A-10
A.17	First principal stress in europium oxide die with 0.003 in. interference fit.....	A-11
A.18	First principal stress in europium oxide die with 0.002 in. interference fit.....	A-11
A.19	First principal stress in europium oxide die with 0.001 in. interference fit.....	A-12
A.20	Second principal stress in europium oxide die with 0.004 in. interference fit	A-12
A.21	Second principal stress in europium oxide die with 0.003 in. interference fit	A-13
A.22	Second principal stress in europium oxide die with 0.002 in. interference fit	A-13
A.23	Second principal stress in europium oxide die with 0.001 in. interference fit	A-14
A.24	Third principal stress in europium oxide die with 0.004 in. interference fit	A-14
A.25	Third principal stress in europium oxide die with 0.003 in. interference fit	A-15
A.26	Third principal stress in europium oxide die with 0.002 in. interference fit	A-15
A.27	Third principal stress in europium oxide die with 0.001 in. interference fit	A-16
A.28	First principal stress in tantalum die with 0.01 in. interference fit.....	A-16
A.29	First principal stress in tantalum die with 0.006 in. interference fit.....	A-17
A.30	First principal stress in tantalum die with 0.004 in. interference fit.....	A-17
A.31	First principal stress in tantalum die with 0.002 in. interference fit.....	A-18
A.32	First principal stress in tantalum die with 0.001 in. interference fit.....	A-18
A.33	Second principal stress in tantalum die with 0.01 in. interference fit	A-19
A.34	Second principal stress in tantalum die with 0.006 in. interference fit	A-19
A.35	Second principal stress in tantalum die with 0.004 in. interference fit	A-20
A.36	Second principal stress in tantalum die with 0.002 in. interference fit	A-20

A.37	Second principal stress in tantalum die with 0.001 in. interference fit.....	A-21
A.38	Third principal stress in tantalum die with 0.01 in. interference fit.....	A-21
A.39	Third principal stress in tantalum die with 0.006 in. interference fit.....	A-22
A.40	Third principal stress in tantalum die with 0.004 in. interference fit.....	A-22
A.41	Third principal stress in tantalum die with 0.002 in. interference fit.....	A-23
A.42	Third principal stress in tantalum die with 0.001 in. interference fit.....	A-23
A.43	First principal stress in tantalum die with 0.002 in. interference fit	A-24
A.44	First principal stress in tantalum die with 0.001 in. interference fit	A-24
A.45	First principal stress in tantalum die with no interference fit	A-25
A.46	Second principal stress in tantalum die with 0.002 in. interference fit.....	A-25
A.47	Second principal stress in tantalum die with 0.001 in. interference fit.....	A-26
A.48	Second principal stress in tantalum die with no interference fit.....	A-26
A.49	Third principal stress in tantalum die with 0.002 in. interference fit.....	A-27
A.50	Third principal stress in tantalum die with 0.001 in. interference fit.....	A-27
A.51	Third principal stress in tantalum die with no interference fit.....	A-28
A.52	First principal stress in europium oxide die with 0.0055 in. inner corner radius.....	A-28
A.53	First principal stress in europium oxide die with 0.0030 in. inner corner radius.....	A-29
A.54	Second principal stress in europium oxide die with 0.0055 in. inner corner radius	A-29
A.55	Second principal stress in europium oxide die with 0.0030 in. inner corner radius	A-30
A.56	Third principal stress in europium oxide die with 0.0055 in. inner corner radius	A-30
A.57	Third principal stress in europium oxide die with 0.0030 in. inner corner radius	A-31
A.58	First principal stress in europium oxide die with 240,000 lb applied.....	A-31
A.59	First principal stress in europium oxide die with 224,000 lb applied.....	A-32
A.60	Second principal stress in europium oxide die with 240,000 lb applied	A-32
A.61	Second principal stress in europium oxide die with 224,000 lb applied	A-33
A.62	Third principal stress in europium oxide die with 240,000 lb applied	A-33
A.63	Third principal stress in europium oxide die with 224,000 lb applied	A-34
A.64	First principal stress in tantalum die with 100,000 lb applied.....	A-34
A.65	First principal stress in tantalum die with 78,000 lb applied.....	A-35
A.66	Second principal stress in tantalum die with 100,000 lb applied	A-35
A.67	Second principal stress in tantalum die with 78,000 lb applied	A-36
A.68	Third principal stress in tantalum die with 100,000 lb applied	A-36
A.69	Third principal stress in tantalum die with 78,000 lb applied	A-37
A.70	First principal stress in europium oxide die with original geometry.....	A-37
A.71	First principal stress in europium oxide die with cavity size increased by 0.002 in. per side.....	A-38
A.72	Second principal stress in europium oxide die with original geometry	A-38
A.73	Second principal stress in europium oxide die with cavity size increased by 0.002 in. per side.....	A-39
A.74	Third principal stress in europium oxide die with original geometry	A-39
A.75	Third principal stress in europium oxide die with cavity size increased by 0.002 in. per side.....	A-40
A.76	First principal stress in europium oxide die with original geometry.....	A-40
A.77	First principal stress in europium oxide die with tantalum die's outer radius geometry.....	A-41
A.78	Second principal stress in europium oxide die with original geometry	A-41
A.79	Second principal stress in europium oxide die with tantalum die's outer radius geometry.....	A-42
A.80	Third principal stress in europium oxide die with original geometry	A-42

A.81	Third principal stress in europium oxide die with tantalum die's outer radius geometry	A-43
------	---	------

LIST OF TABLES

Table		Page
1	Max stress and distortion in europium oxide two-piece die.....	8
2	Max stress and distortion in tantalum two-piece die.....	9
3	Effect of decreased corner radius on stresses in europium oxide die.....	10
4	Effect of decreased compressive force on stresses in europium oxide die.....	10
5	Effect of decreased compressive force on stresses in tantalum die	10
6	Effect of increased cavity size on stresses in europium oxide die.....	11
7	Effect of outer ring geometry on stresses in europium oxide die	11

ABSTRACT

Compaction dies used to create europium oxide and tantalum control plates were modeled using ANSYS 11.0.¹ Two-piece designs were considered in order to make the dies easier to assemble than the five-piece dies that were previously used. The two areas of concern were the stresses at the interior corner of the die cavity and the distortion of the cavity wall due to the interference fit between the two pieces and the pressure exerted on the die during the compaction process. A successful die design would have stresses less than the yield stress of the material and a maximum wall distortion on the order of 0.0001 in. Design factors that were investigated include the inner corner radius, the value of the interference fit, the compaction force, the size of the cavity, and the outer radius and geometry of the outer ring.

The results show that for the europium oxide die, a 0.01 in. diameter wire can be used to create the cavity, leading to a 0.0055 in. radius corner, if the radial interference fit is 0.003 in. For the tantalum die, the same wire can be used with a radial interference fit of 0.001 in. Also, for the europium oxide die with a 0.003 in. interference fit, it is possible to use a wire with a diameter of 0.006 in. for the wire burning process.

Adding a 10% safety factor to the compaction force tends to lead to conservative estimates of the stresses but not for the wall distortion. However, when the 10% safety factor is removed, the wall distortion is not affected enough to discard the design. Finally, regarding the europium oxide die, when the cavity walls are increased by 0.002 in. per side or the outer ring is made to the same geometry as the tantalum die, all the stresses and wall distortions are within the desired range. Thus, the recommendation is to use a 0.006 in. diameter wire and a 0.003 in. interference fit for the europium oxide die and a 0.01 in. diameter wire and a 0.001 in. interference fit for the tantalum die. The dies can also be made to have the same outer geometry if desired.

1. INTRODUCTION

Many of the metallic control plates used in nuclear reactors are produced through a powder compaction process. This involves compressing metallic powder at very high pressures in a die until a solid piece in the shape of the die is formed. Some of the control plates that are currently being used have been in use since the 1950s and are suffering from wear. Since manufacturing processes have improved significantly since the 1950s, it is possible to design a simpler, more manufacturable die to produce the same result.

The control plates being produced by these dies are rectangular, and in order to create sharp edges on the plates, the dies that made them in the 1950s consisted of five pieces. A schematic of this “five-piece” design can be seen in Fig. 1.

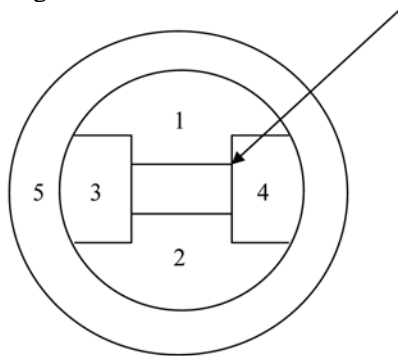


Fig. 1. Schematic of “five-piece” powder compression die.

The parts labeled 1–4 were bolted together, and in an effort to minimize the stresses to the die during the compaction process, part 5 was added with an interference fit around the outer edge of the die. The meaning of “interference fit” is means that the inner radius of part 5 would be somewhat smaller than the outer radius of the die insert created by parts 1–4. Part 5 would then be heated, causing it to expand, and in this state it would be placed around the outside of the die insert. When the part cooled, it would revert to its original dimensions, causing the die insert to be in a state of compressive stress in its normal condition. Thus, when the compaction process is creating large stresses in the interior of the die, the die is in a less stressed and less distorted state. The amount of interference fit can be adjusted in order to minimize the distortion of the die’s interior walls during compaction, creating control plates with the desired dimensions.

Modern manufacturing processes have evolved such that it is not necessary to have such a complicated die. Recall that the five-piece die was created in order to ensure that the interior corners (one of which is denoted with an arrow in Fig. 1) were square corners and that the plate had sharp edges. With current wire-burning manufacturing techniques, manufacturers can use a small radius wire to create interior corners with radii of 0.003 in. or smaller. This ability negates the need for a complex five-piece die and allows manufacturers to replace the insert composed of parts 1–4 in Fig. 1 with a single piece. This design will be referred to as a “two-piece” die and is shown schematically in Fig. 2.

The two-piece design is obviously less complex. The purpose of this study is to determine the localized stresses felt in the interior corners (e.g., the one pointed out in Fig. 2) and to determine the optimum value of interference fit between parts 1 and 2 in order to minimize the stresses and the distortion of the interior walls of the die during compaction.

Two dies were considered: one for compacting europium oxide powder and another for compacting tantalum powder.

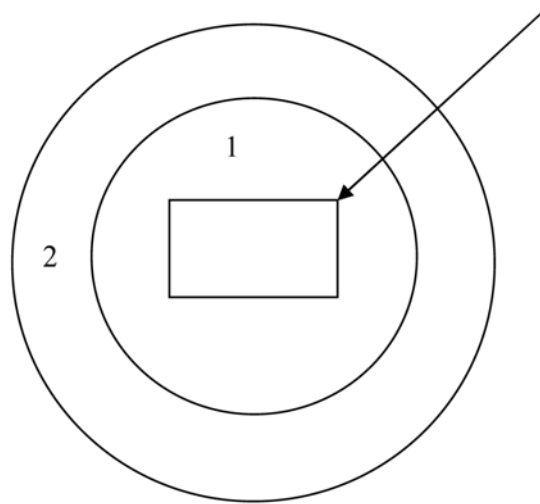


Fig. 2. Schematic of “two-piece” powder compression die.

1.1 DIE MODELS

Although each of the two die models took the two-piece form, based on the dies they were being designed to replace, they had different geometries. Figure 3 shows the two die models. Note that there is a step in the outer ring of the europium oxide die, which is denoted by the dotted line. Most of the analyses were done using the geometry of the original dies, but since the more complex geometry of the europium oxide die was not a requirement, the final step of this study investigated the effect of creating the europium oxide die with the outer ring geometry of the tantalum die.

1.1.1 Geometry and Materials

The nominal dimensions are as follows: For the europium oxide die [Fig. 3(a)], the inner cavity is 3.4552×1.7246 in. The outer diameter of the insert is 5.960 in., and the outer diameter of the outer ring is 7.940 in. The step, which is 0.252 in. deep, occurs at a diameter of 7.050 in. The die, with the exception of the stepped portion, is 3.02 in. deep. The stepped portion is 2.516 in. deep.

For the tantalum die [Fig. 3(b)], the inner cavity is 3.4640×0.8086 in. The outer diameter of the insert is 6.150 in., and the outer diameter of the outer ring is 8.150 in. The die is 2.960 in. deep.

Both dies were modeled with the same materials. The die insert is made of AISI-D2-TS steel and heat treated to a Rockwell C hardness of 58 to 60. The outer ring is made of 4340 steel and heat treated to a Rockwell C hardness of 28 to 32. The properties of both the insert and the outer ring were given as an elastic modulus of 30×10^6 psi and a Poisson's Ratio of 0.3. The insert has a yield strength of 312 ksi, and the outer ring has a yield strength of 120 ksi.

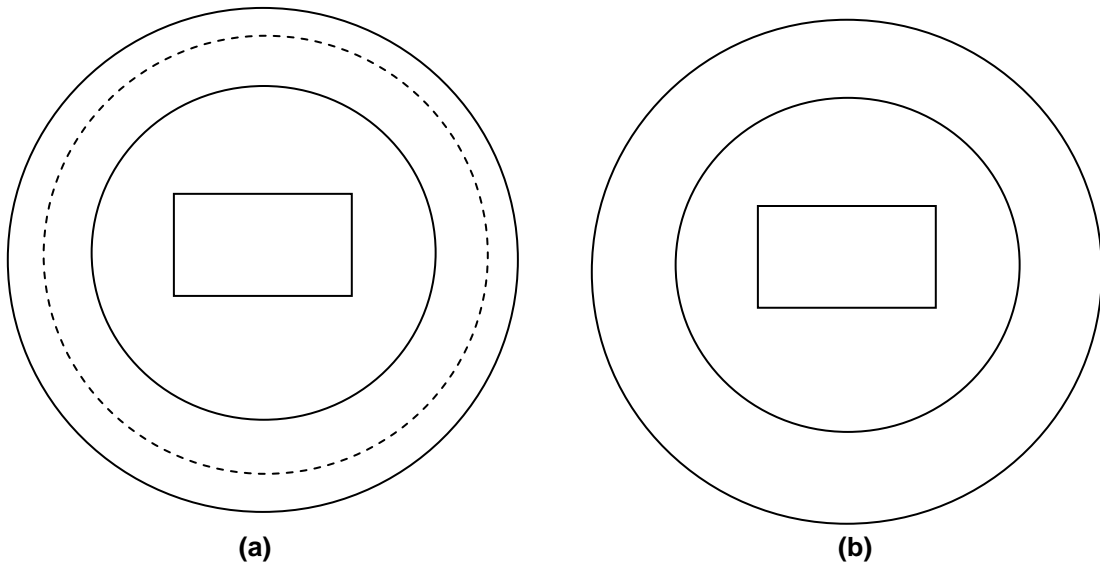


Fig. 3. Schematic of (a) europium oxide and (b) tantalum dies.

1.1.2 Model

In the interest of time and simplicity, one-fourth of each assembly was modeled, and symmetry boundary conditions were used on the “cut” faces to simulate the missing parts of the die. Figure 4 shows the europium oxide die model, and Fig. 5 shows the tantalum die model. The red arrows indicated the corner of interest in this analysis, where stress concentrations could occur and cause the die insert to yield.

The finite-element program ANSYS 11.0 was used, with solid brick95 elements being used for both the die insert and outer ring. To model the interference fit influence, the insert was modeled with the correct outer diameter and the outer ring was modeled with a slightly smaller inner diameter, forcing the pieces to overlap. Contact elements were created between the inside face of the outer ring and the outside face of the insert. This effect simulated the compression created on the insert by the interference fit with the outer ring. The mesh was done by sweeping the solids with a tetrahedral mesh.

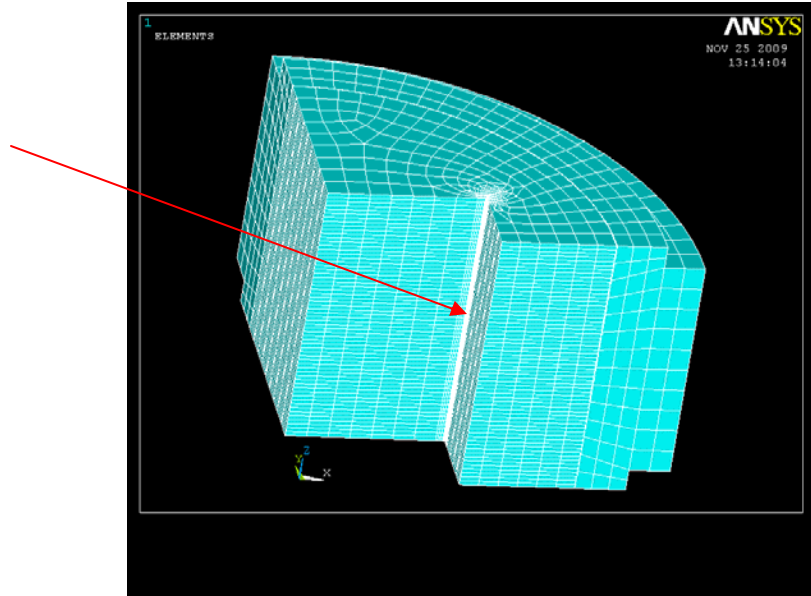


Fig. 4. Finite-element model of europium oxide die.

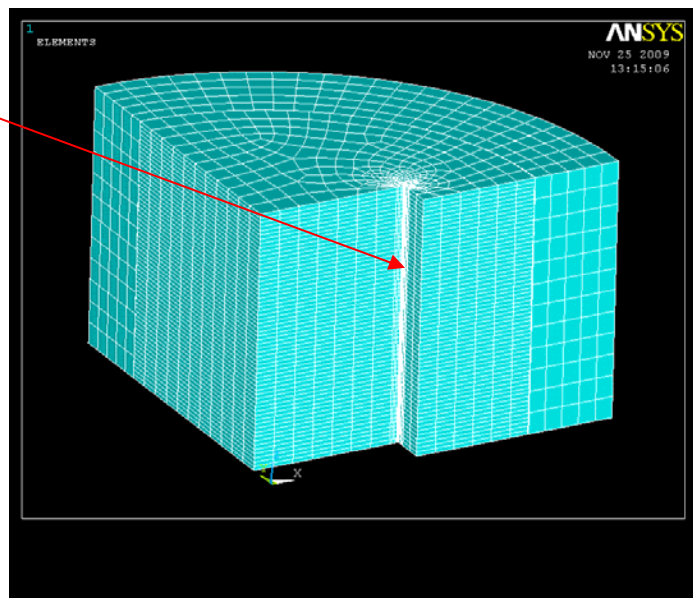


Fig. 5. Finite-element model of tantalum die.

1.1.3 Loading

The two scenarios that were simulated were the “no load” condition, where the only influence is the interference fit between the two pieces, and the “loaded” condition, where the die was undergoing the powder compaction process, causing a large pressure to build up along the walls of the inner cavity. The maximum compressive force was used for both dies, and it was assumed that this force caused a constant hydrostatic pressure across the middle 0.525 in. of the die, since the final compacts were to be 0.525 in. deep. For the europium oxide die, the maximum force was 240,000 lb, creating a

pressure of 44,128 psi on the cavity wall. For the tantalum die, the maximum force was 100,000 lb, creating a pressure of 22,290 psi on the cavity wall.

2. INNER CORNER RADIUS

2.1 DISCUSSION

The first set of simulations was intended to determine what diameter wire could be used in the wire burning process to create an inner corner with acceptably low stresses while still creating relatively sharp edges on the final compact. In these simulations, the radial interference fit was held constant at 0.01 in.*

2.2 RESULTS

The wire diameter being discussed for use in this situation was 0.01 in., which could create an inner corner with a 0.0055 in. radius. When this radius was used on the two-piece dies, extremely large pressures occurred at the corner. In the no load condition, the maximum compressive stress in the europium oxide die was 620 ksi and in the tantalum die it was 674 ksi, which are both well above the 312 ksi yield strength of the die insert. Figures 6 and 7 show typical stress distributions at the inner corner being discussed.

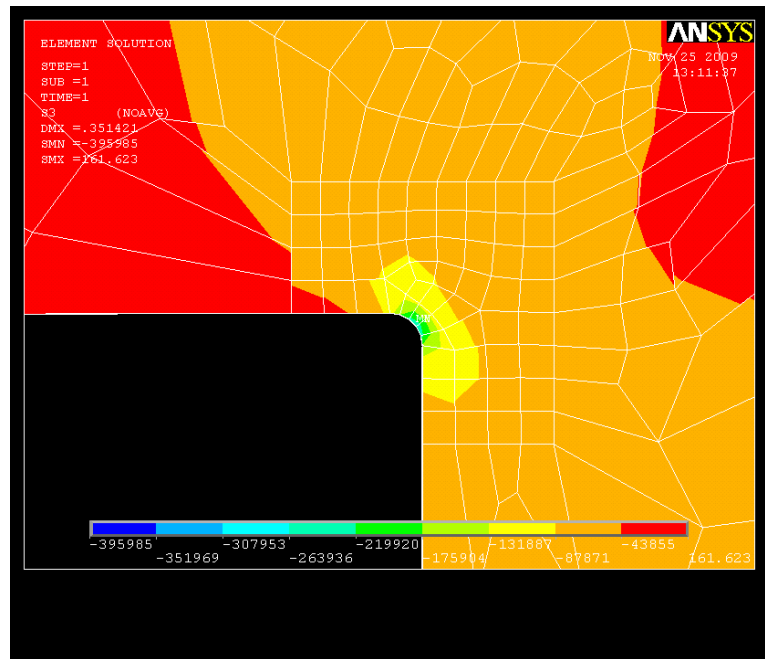


Fig. 6. Stress distribution in corner (top view).

*The values of interference fit given in this report are radial values, not diametrical values. Therefore, for a reported interference fit of 0.01 in., the inner diameter of the outer ring would be 0.02 in. smaller than the outer diameter of the die insert.

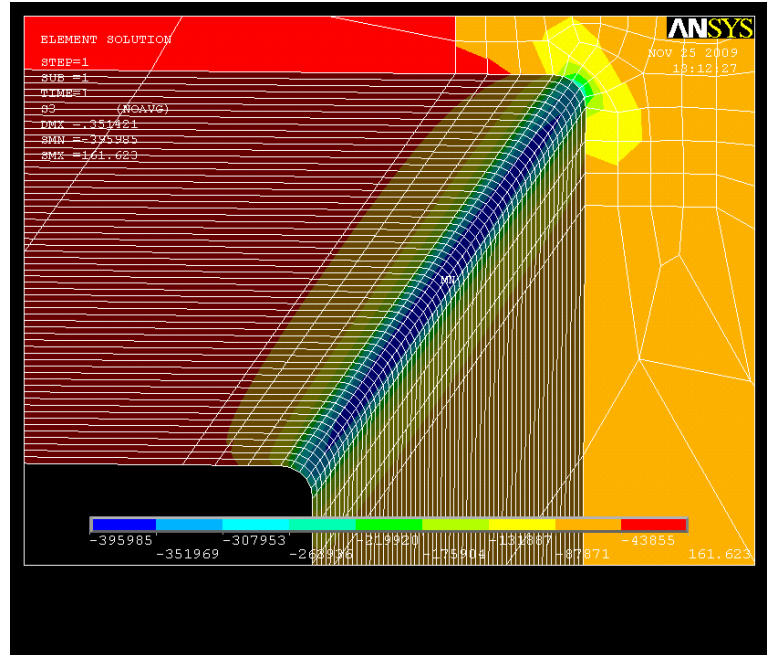


Fig. 7. Stress distribution in corner (skew view).

Since the 0.0055 in. radius created such high local stresses, larger diameter wires were investigated. The radius of the corner was increased to 0.012 in. and to 0.025 in. in order to see if the stresses were more manageable. For the europium oxide die, the 0.012 in. radius yielded a maximum compressive stress of 492 ksi and the 0.025 in. radius yielded a maximum compressive stress of 396 ksi. For the tantalum die, the maximum compressive stress for the 0.012 in. radius corner was 442 ksi and for the 0.025 in. radius it was 358 ksi. All of these stresses were found in the no load condition. Also, all of these stresses are above the yield stress of 312 ksi, so wire burning with a 0.01 in. interference fit would not be advised.

3. INTERFERENCE FIT*

3.1 DISCUSSION

Because it was previously found that a 0.01 in. radial interference fit caused unacceptable stress levels in a two-piece die formed by wire burning, the effect of reducing the interference fit was studied. The high stress levels were compressive stresses in the small radius corner, caused by the pressure exerted by the outer ring on the insert. By reducing the value of the interference fit, it is possible to reduce the stress in the corner of interest.

When deciding on the optimum value for the interference fit between the two pieces of a die, there were two considerations: the maximum stress at the corner and the maximum distortion of the inner cavity wall. Under the no load condition, the corner will experience high compressive stresses as it feels pressure from the outer ring, and the inner cavity walls will bend in under that pressure. When the compaction load is applied, some of the compressive load is relieved in the corner due to the hydrostatic pressure applied during the compaction process. Also, that pressure tends to push back on the cavity wall, generally reducing the distortion of the wall that was caused by the interference fit. The

*All of the stress contour plots for the simulations being discussed can be found in Appendix A.

goal of this set of simulations was to determine an optimal value of interference fit for both two-piece dies, assuming a 0.0055 in. radius for the inside corner.

3.2 RESULTS

Figure 8 shows the initial results, which are the maximum stresses at the inside corner as a function of the interference fit for both dies. These stresses are in the no load condition, and the graph shows that an interference fit of less than 0.006 in. is required to remain below the yield strength of the die insert.

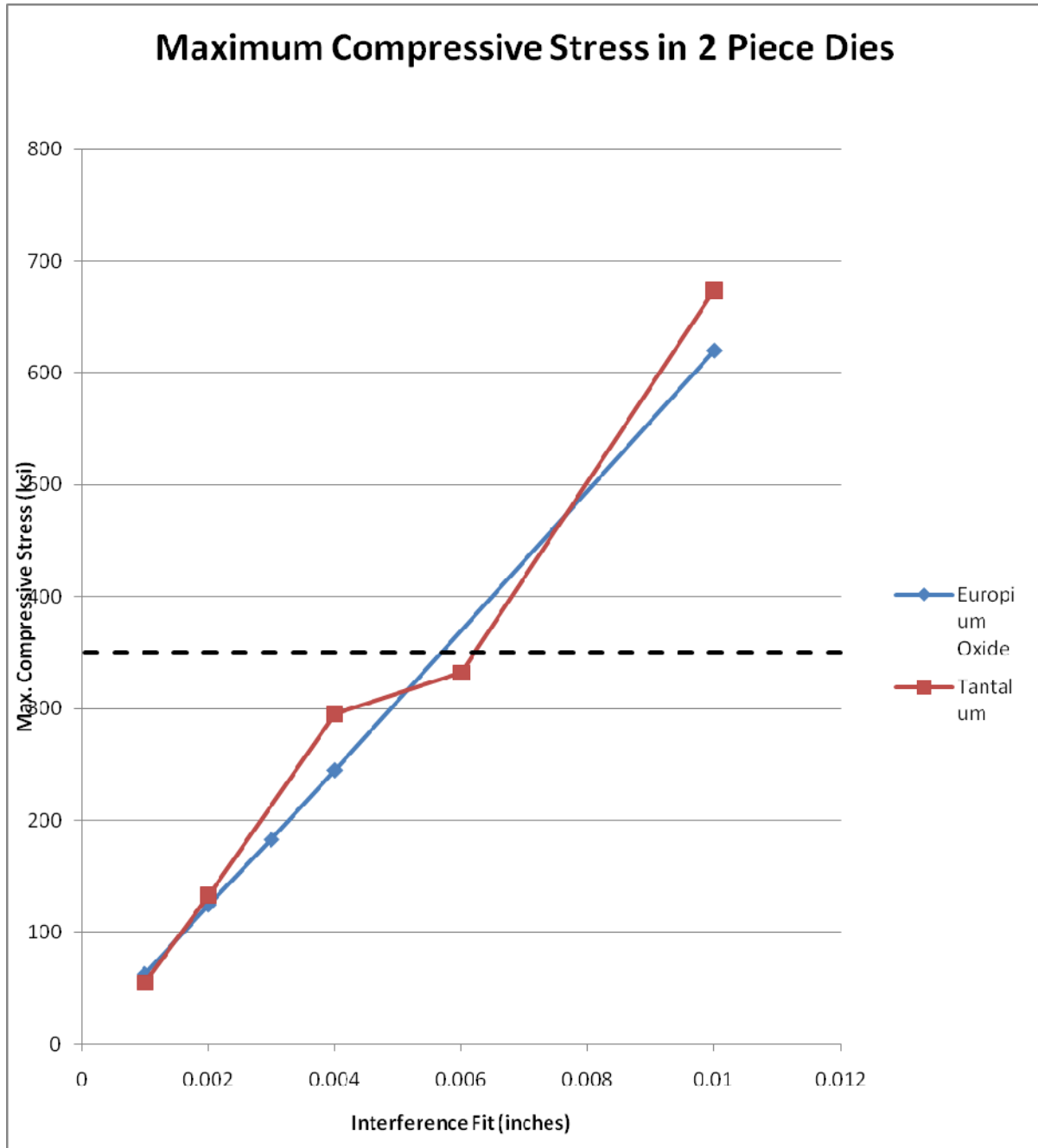


Fig. 8. Maximum stress vs interference fit.

In addition, in order for the compact to be correctly dimensioned and easily removed from the die, the distortion of the wall should be minimized. Figure 9 shows where the wall distortion is at a maximum, and therefore indicates where the distortion was measured.

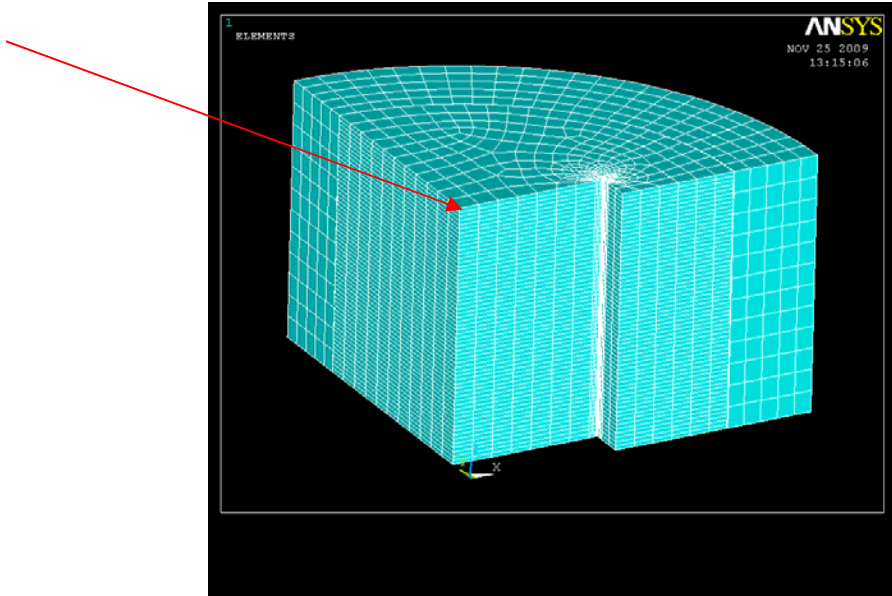


Fig. 9. Area of maximum wall distortion in tantalum die.

Table 1 shows the results from several trials of different interference fits of the europium oxide die under the no load and the loaded conditions.

Table 1. Max stress and distortion in europium oxide two-piece die

Interference fit (in.)	Europium oxide			
	No load		Loaded	
	Max stress (ksi)	Max distortion (in.)	Max stress (ksi)	Max distortion (in.)
0.004	245	0.001857	248	0.000676
0.003	183	0.001393	309	0.000211
0.002	125	0.000928	381	0.000256
0.001	63	0.000463	443	(+)0.000721

Table 2 shows the results from several trials of different interference fits of the tantalum die under the no load and the loaded conditions.

As can be seen in Table 2, a good choice of interference fit for the tantalum die is 0.001 in. The stresses are very small under the no load condition, and when loaded the maximum stress is still well below the yield strength of the material. The goal for maximum distortion of the inner wall under load was 0.0001 in., and this is nearly achieved with an interference fit of 0.001 in. in the tantalum die.

Table 2. Max stress and distortion in tantalum two-piece die

Interference fit (in.)	Tantalum			
	No load		Loaded	
	Max stress (ksi)	Max distortion (in.)	Max stress (ksi)	Max distortion (in.)
0.002	133	0.0008	130	0.000282
0.001	55	0.0004	185	0.000119
0			268	

It is somewhat more difficult to determine the optimum value for the interference fit in the two-piece europium oxide die. With a 0.001 in. interference fit, the no load stress is small, but it is not enough to counteract the additional stress added by the compaction process. The positive sign in front of the maximum distortion under load in the 0.001 in. interference fit case means that under load, the pressure is enough to actually cause the inner wall to deform in the opposite direction, or out, towards the outer ring.

Additionally, there are trade-offs between an interference fit of 0.002 in. and 0.003 in. in the europium oxide die. The advantage of the 0.002 in. interference fit is that the distortion and maximum stress under no load are both smaller than in the case of a 0.003 in. interference fit. However, during the compaction process, the small pressure exerted by the outer ring is not enough to counteract the compaction pressure, resulting in very high stresses. For the 0.003 in. interference fit, the distortion and maximum stress with no load are larger, but during compaction the maximum stress and distortion are smaller, and the stress is below the material's yield strength. The goal of 0.0001 in. maximum wall distortion is not achieved, but it appears that a 0.003 in. radial interference fit is the best choice for the design of the europium oxide die.

4. ADDITIONAL STUDIES

4.1 SMALLER WIRE DIAMETER

One additional consideration is that 0.01 in. diameter is not the smallest possible wire for use in the wire burning process. A smaller radius for the inner corner of the insert is possible by using a smaller wire. The goal of this set of simulations was to determine if using a smaller diameter wire would result in significantly higher stresses. This study was done with the europium oxide die with an interference fit of 0.003 in.

The result of this study is that if the radius of the inside corner of the insert is reduced from 0.0055 in. to 0.0030 in. (a conservative estimate for a 0.006 in. diameter wire), the maximum value of the first principal stress decreases from the previously reported 309 ksi to 257 ksi. The first principal stress is the highest of the three principal stresses in this case, so it is of most concern. The second principal stress remains relatively constant, and the maximum value of the third principal stress increases from 48 ksi to 91 ksi. All of these stresses are under the yield stress of the insert, which is 312 ksi. Therefore, with an interference fit of 0.003 in., a 0.006 in. diameter wire is preferable to a 0.01 in. diameter wire for the wire burning process. Table 3 shows the maximum compressive and tensile stresses in the europium oxide die with the two different corner radii.

Table 3. Effect of decreased corner radius on stresses in europium oxide die

	Max compressive stress (ksi)		Max tensile stress (ksi)	
	0.0055 in.	0.003 in.	0.0055 in.	0.003 in.
1st Principal stress	31	30	309	257
2nd Principal stress	39	38	99	99
3rd Principal stress	68	57	48	91

4.2 SMALLER COMPACTION FORCE

All of the previous analyses were done with a 10% factor of safety in order to achieve conservative results. The maximum compaction force that was simulated for each die was 10% larger than the expected actual compaction force. The purpose of this set of simulations was to determine what the effect on stresses and wall distortion would be if that 10% factor of safety was removed. The reason this could be an issue is that the compaction pressure reduces the wall distortion caused by the interference fit, and if the actual internal hydrostatic pressure is smaller than in the simulation, the wall distortion during the compaction process may be larger than expected. These simulations were done with the optimal value of interference fit (0.003 in. for the europium oxide die and 0.001 in. for the tantalum die) and an inner corner radius of 0.0055 in.

When the applied force in the europium oxide die was reduced from 240,000 lb to 224,000 lb, the maximum distortion of the inner cavity wall increased from 0.000211 in. to 0.000288 in. However, when the applied force in the tantalum die was reduced from 100,000 lb to 78,000 lb, the maximum distortion of the inner cavity wall decreased from 0.000119 in. to a negligible 0.0000042 in. Therefore, in these cases, removing the safety factor has no significant negative effect on wall distortion in the interior of the die. Table 4 shows the maximum compressive and tensile stresses in the europium oxide die with two compressive forces, and Table 5 shows the same information for the tantalum die.

Table 4. Effect of decreased compressive force on stresses in europium oxide die

	Max compressive stress (ksi)		Max tensile stress (ksi)	
	240,000 lb	224,000 lb	240,000 lb	224,000 lb
1st Principal stress	31	29	309	276
2nd Principal stress	39	36	99	88
3rd Principal stress	68	73	48	42

Table 5. Effect of decreased compressive force on stresses in tantalum die

	Max compressive stress (ksi)		Max tensile stress (ksi)	
	100,000 lb	78,000 lb	100,000 lb	78,000 lb
1st Principal stress	16	12	185	132
2nd Principal stress	20	15	58	42
3rd Principal stress	29	23	32	22

4.3 LARGER INNER CAVITY

Another factor that could influence the results, especially the cavity wall distortion, is that the final size of the cavity for the europium oxide die had not been decided on yet. There was still the

possibility that the size of the cavity could increase by up to 0.002 in. per side, so simulations were run to see what would happen to the stresses and the cavity wall distortion if the cavity was 0.002 in. larger on each side. These simulations were run on the europium oxide die with an interference fit of 0.003 in. and an inner corner radius of 0.0055 in.

When the cavity size was increased, the maximum displacement of the cavity wall increased from 0.000211 in. to 0.000804 in. and all the stresses became more compressive. The changes in maximum compressive and tensile stresses can be seen in Table 6. Since the stresses closest to the yield strength of the material are tensile, increasing the cavity size would be beneficial in terms of stress, although it would increase the amount of wall distortion.

Table 6. Effect of increased cavity size on stresses in europium oxide die

	Max compressive stress (ksi)		Max tensile stress (ksi)	
	Small cavity	Large cavity	Small cavity	Large cavity
1st Principal stress	31	35	309	245
2nd Principal stress	39	41	99	75
3rd Principal stress	68	130	48	31

4.4 LARGER OUTER RADIUS

Finally, a simulation was completed in order to determine if modifying the outer ring design for the europium oxide die would have a significant impact on the stresses. The europium oxide outer ring was modified such that its outer radius was the same as the outer radius of the tantalum die (8.150 in.) and, like the tantalum die, had no step on the outer edge. The result of this simulation was that the maximum first principal stress decreased markedly, from 309 ksi to 238 ksi, the second principal stress was similar between the two cases, and the maximum value of the third principal stress increased from 48 ksi to 82 ksi, which is still well below the die insert yield strength of 312 ksi. As with the other simulations, the maximum stress in the outer ring was also much lower than its yield strength of 120 ksi. This simulation showed that the europium oxide die with a 0.003 in. interference fit could be made with the same outer ring geometry as the tantalum die. Table 7 shows the maximum compressive and tensile stresses in the europium oxide die with the original, stepped geometry of the outer ring and with the geometry of the tantalum die.

Table 7. Effect of outer ring geometry on stresses in europium oxide die

	Max compressive stress (ksi)		Max tensile stress (ksi)	
	Orig. geometry	Tantalum geom.	Orig. geometry	Tantalum geom.
1st Principal stress	31	30	309	238
2nd Principal stress	39	39	99	91
3rd Principal stress	68	77	48	82

5. REFERENCES

1. ANSYS Mechanical, Version 11.0, ANSYS Inc., Canonsburg, Pennsylvania, January 2007.

APPENDIX A
PRINCIPAL STRESS CONTOUR CHARTS

APPENDIX A. PRINCIPAL STRESS CONTOUR CHARTS

A.1 MODIFYING INTERFERENCE FIT

The following stress contour plots show europium oxide dies with the original geometry and in the unloaded (no compaction force) condition.

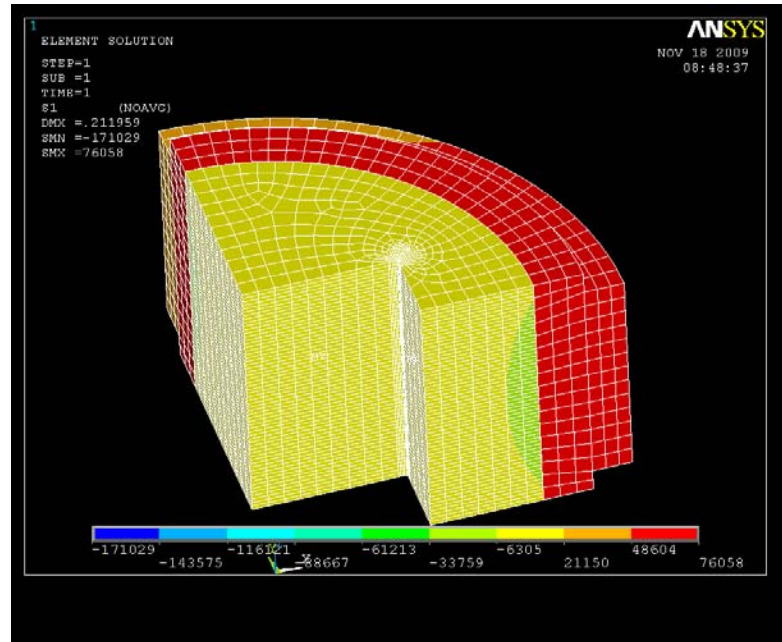


Fig. A.1. First principal stress in europium oxide die with 0.01 in. interference fit.

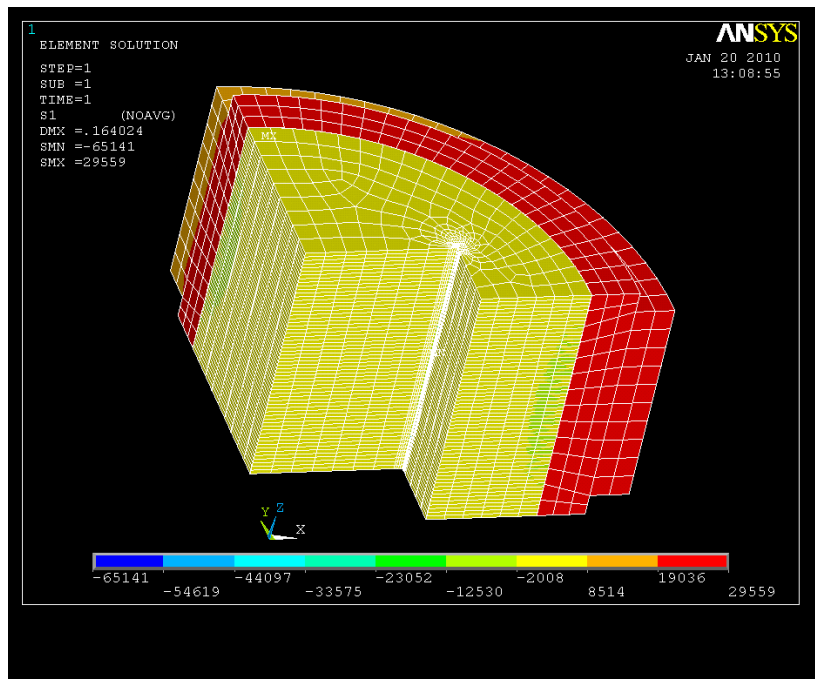


Fig. A.2. First principal stress in europium oxide die with 0.004 in. interference fit.

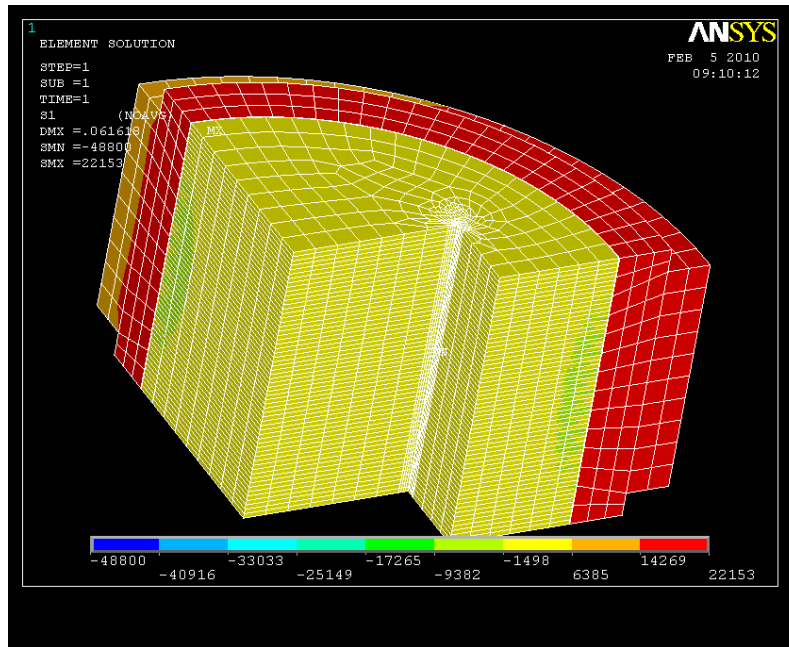


Fig. A.3. First principal stress in europium oxide die with 0.003 in. interference fit.

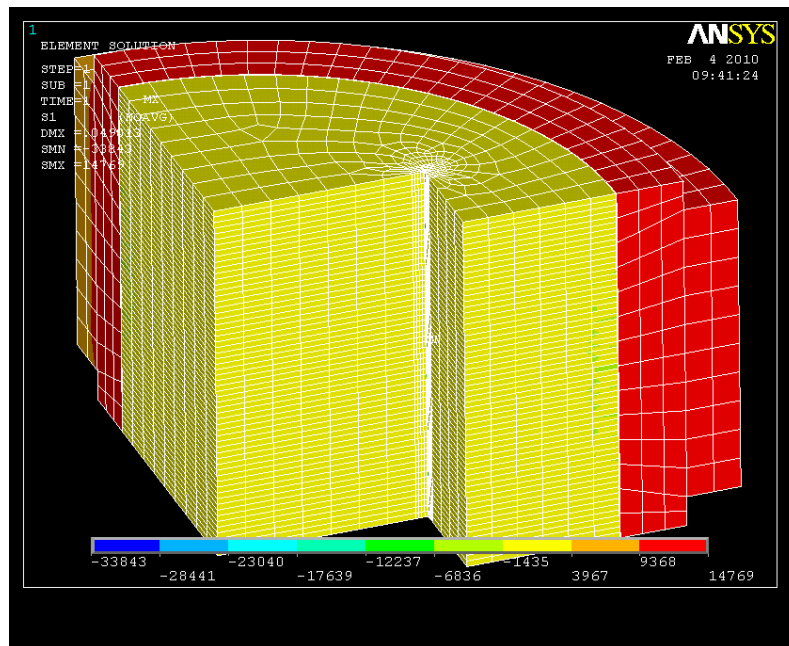


Fig. A.4. First principal stress in europium oxide die with 0.002 in. interference fit.

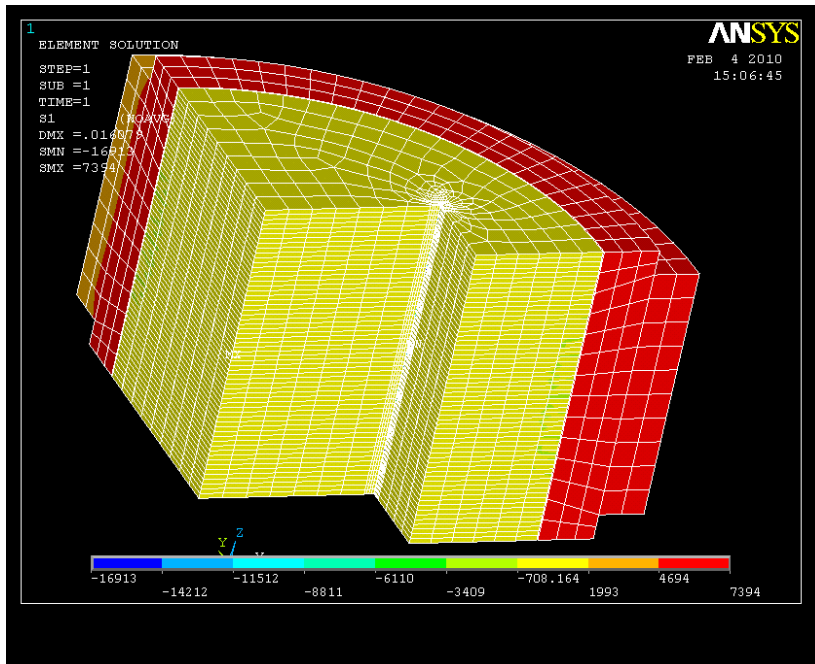


Fig. A.5. First principal stress in europium oxide die with 0.001 in. interference fit.

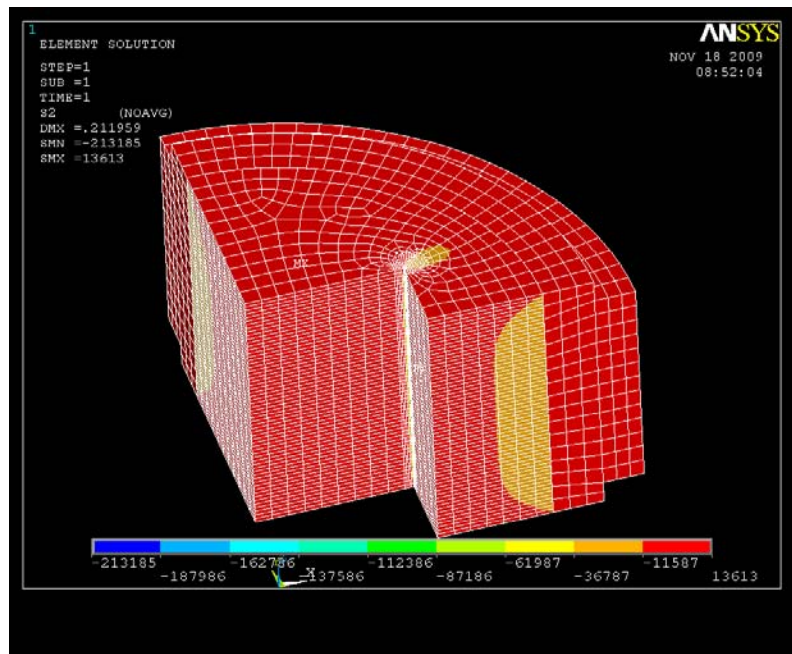


Fig. A.6. Second principal stress in europium oxide die with 0.01 in. interference fit.

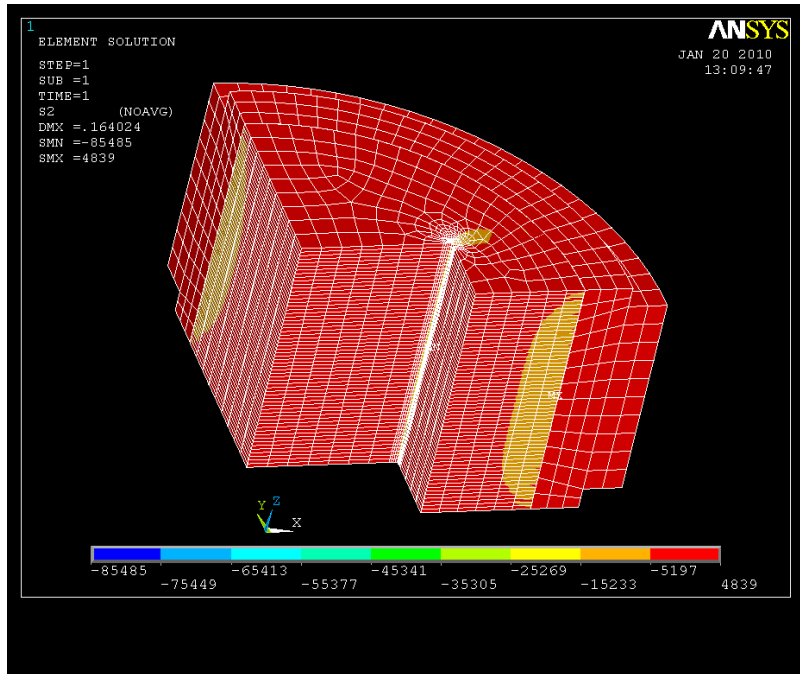


Fig. A.7. Second principal stress in europium oxide die with 0.004 in. interference fit.

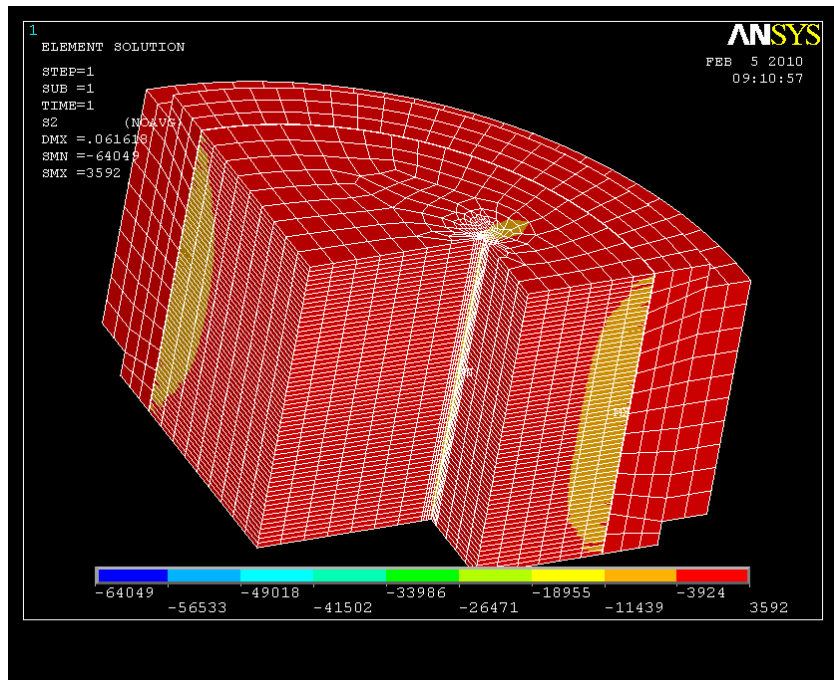


Fig. A.8. Second principal stress in europium oxide die with 0.003 in. interference fit.

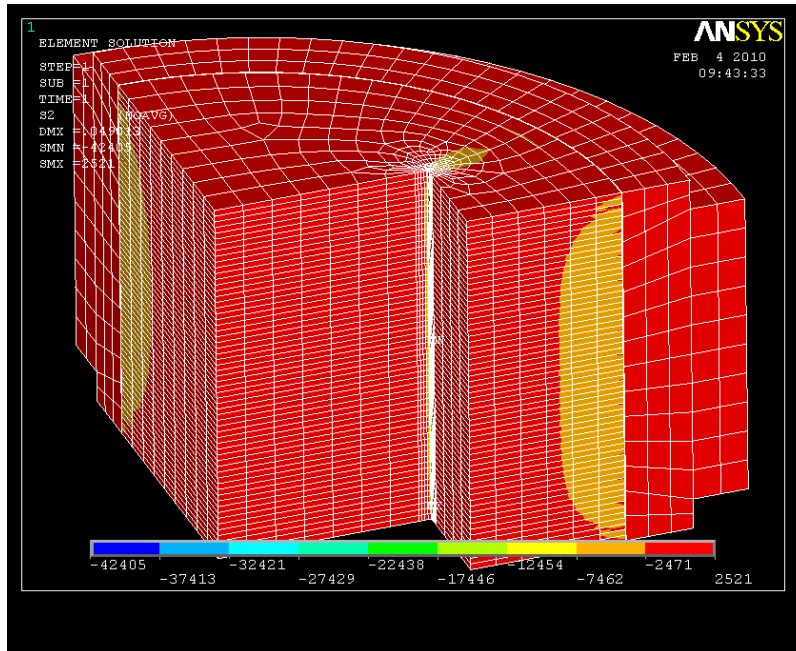


Fig. A.9. Second principal stress in europium oxide die with 0.002 in. interference fit.

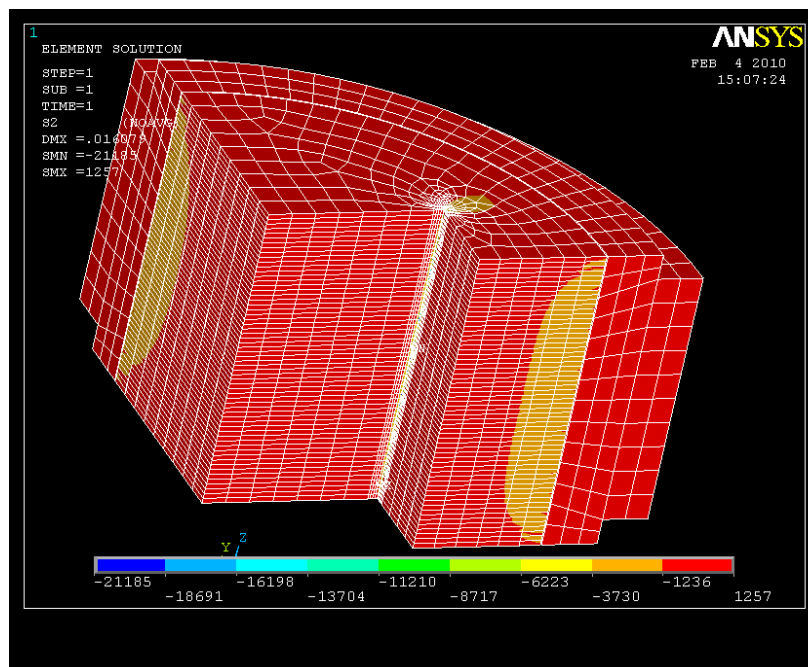


Fig. A.10. Second principal stress in europium oxide die with 0.001 in. interference fit.

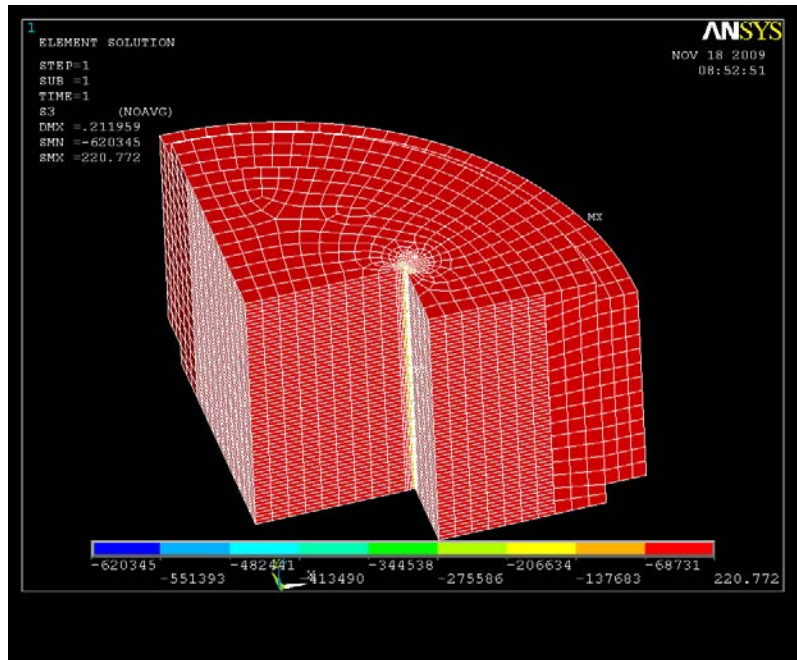


Fig. A.11. Third principal stress in europium oxide die with 0.01 in. interference fit.

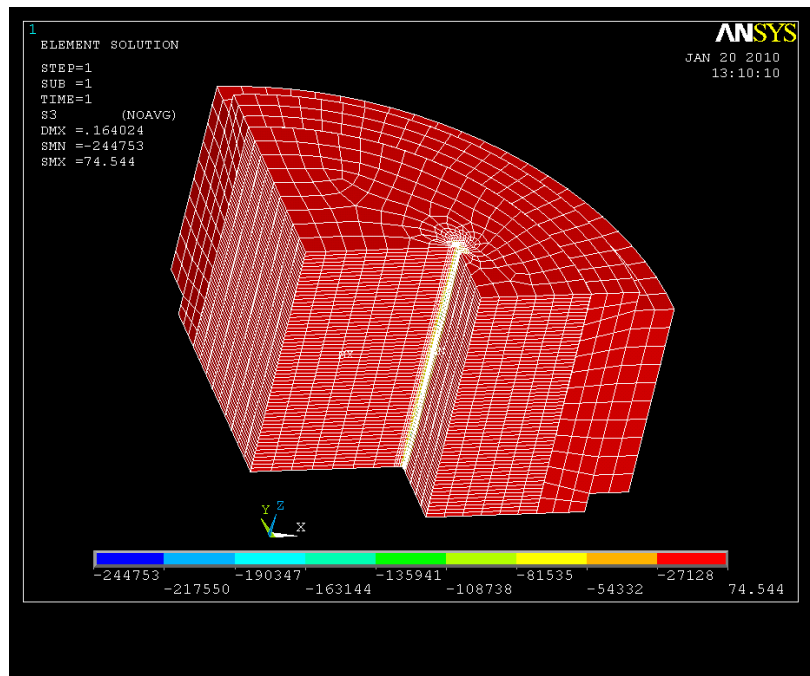


Fig. A.12. Third principal stress in europium oxide die with 0.004 in. interference fit.

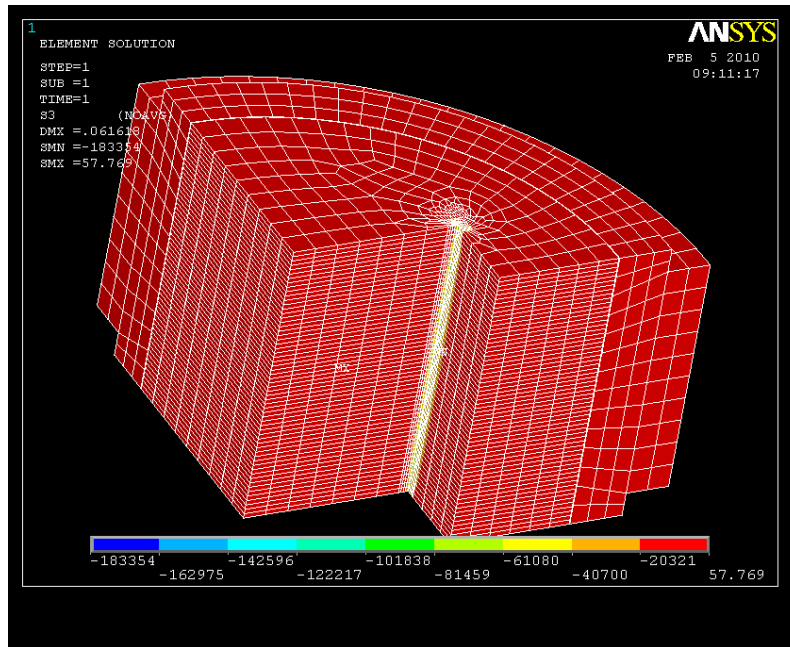


Fig. A.13. Third principal stress in europium oxide die with 0.003 in. interference fit.

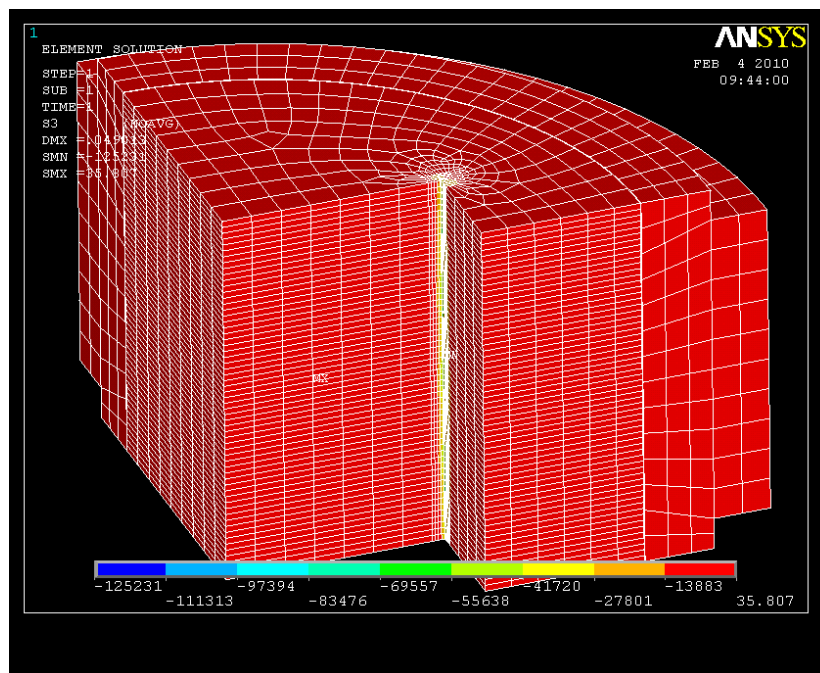


Fig. A.14. Third principal stress in europium oxide die with 0.002 in. interference fit.

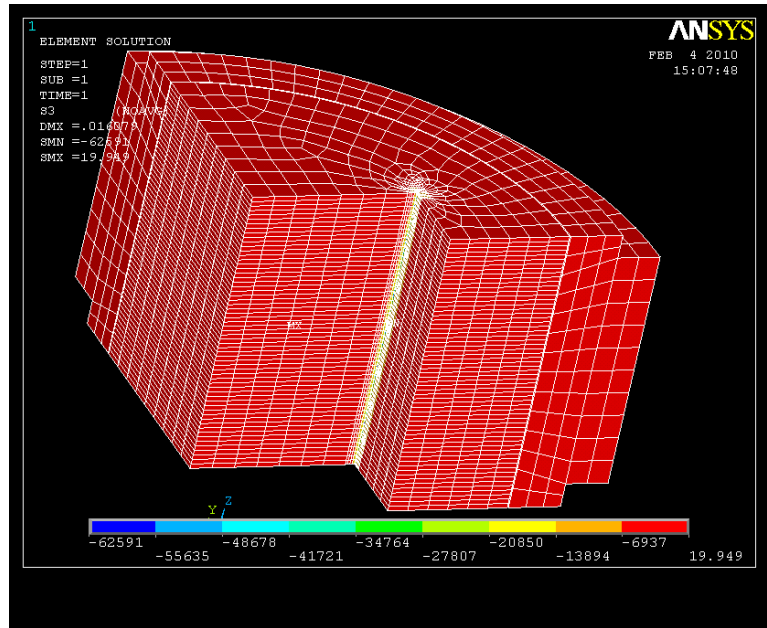


Fig. A.15. Third principal stress in europium oxide die with 0.001 in. interference fit.

The following stress contour plots show europium oxide dies with the original geometry and an applied compaction force of 240,000 lb.

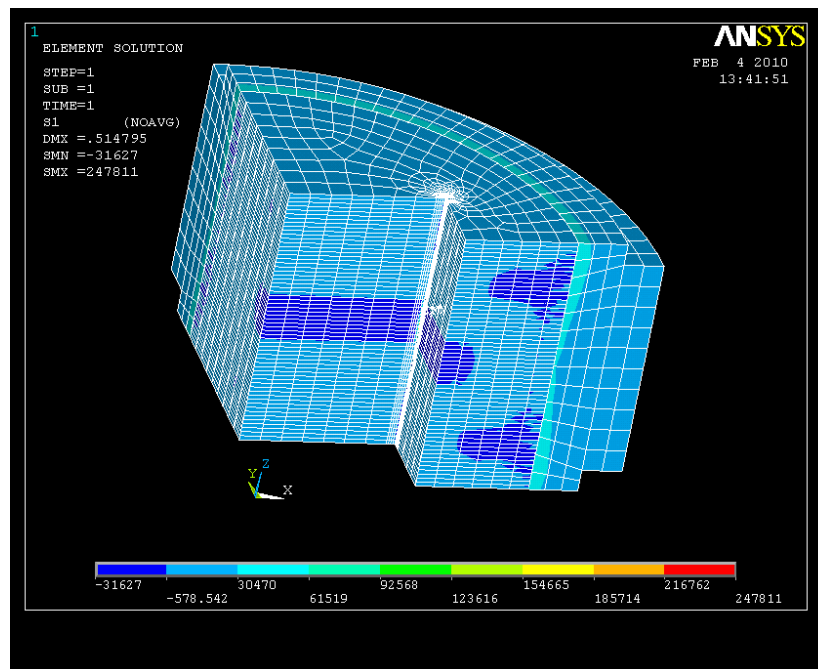


Fig. A.16. First principal stress in europium oxide die with 0.004 in. interference fit.

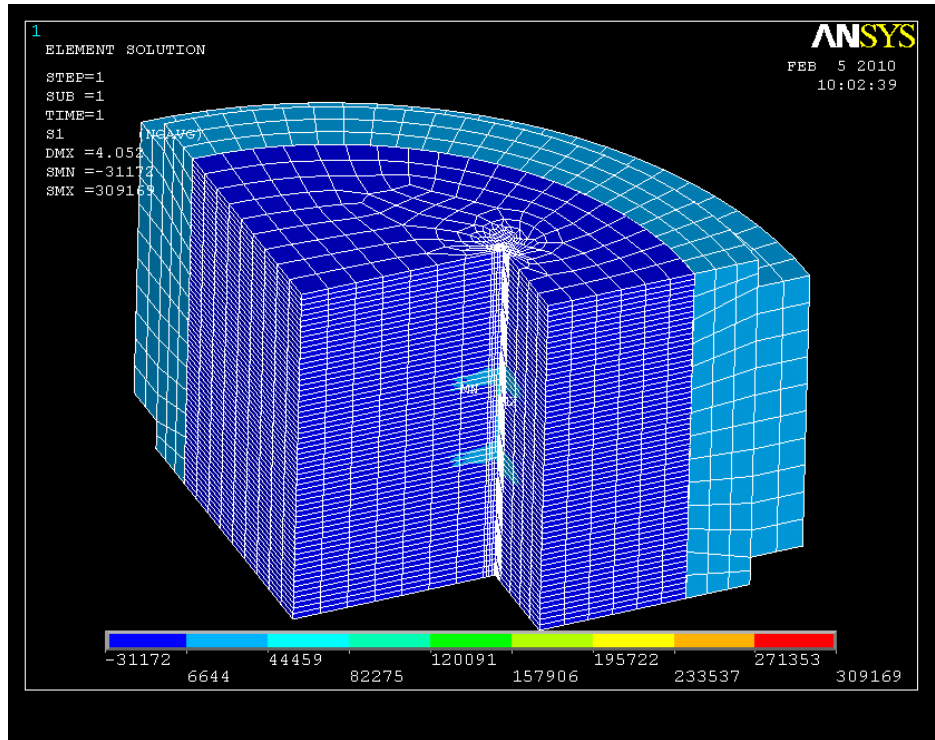


Fig. A.17. First principal stress in europium oxide die with 0.003 in. interference fit.

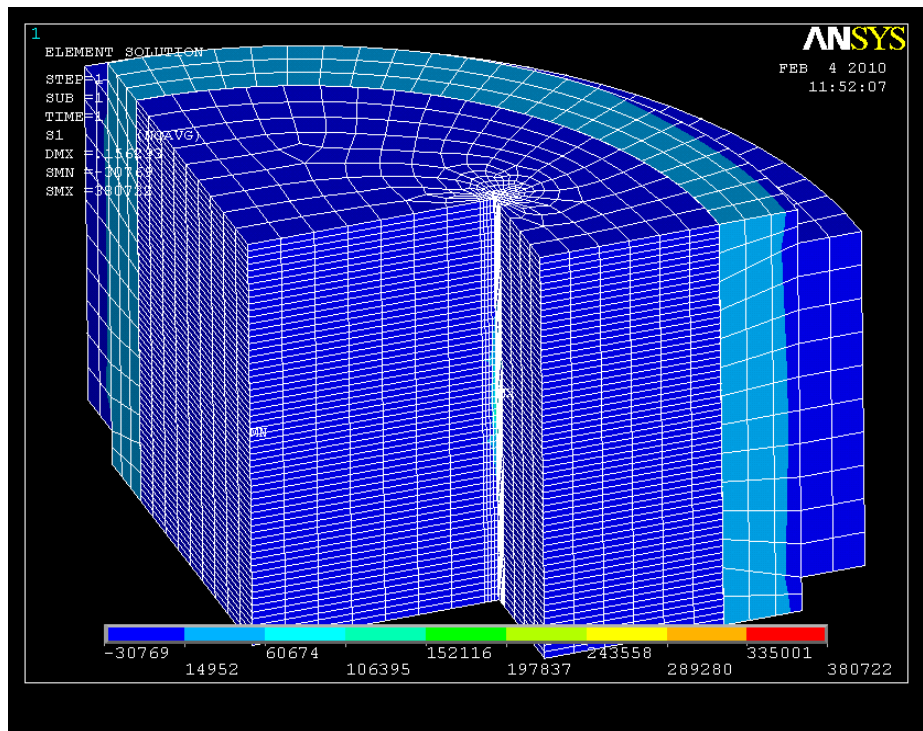


Fig. A.18. First principal stress in europium oxide die with 0.002 in. interference fit.

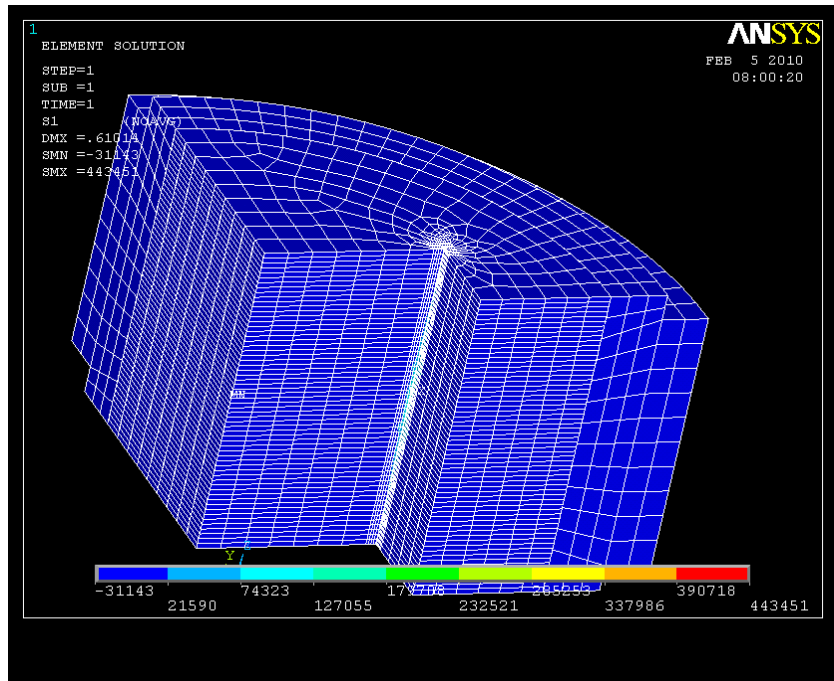


Fig. A.19. First principal stress in europium oxide die with 0.001 in. interference fit.

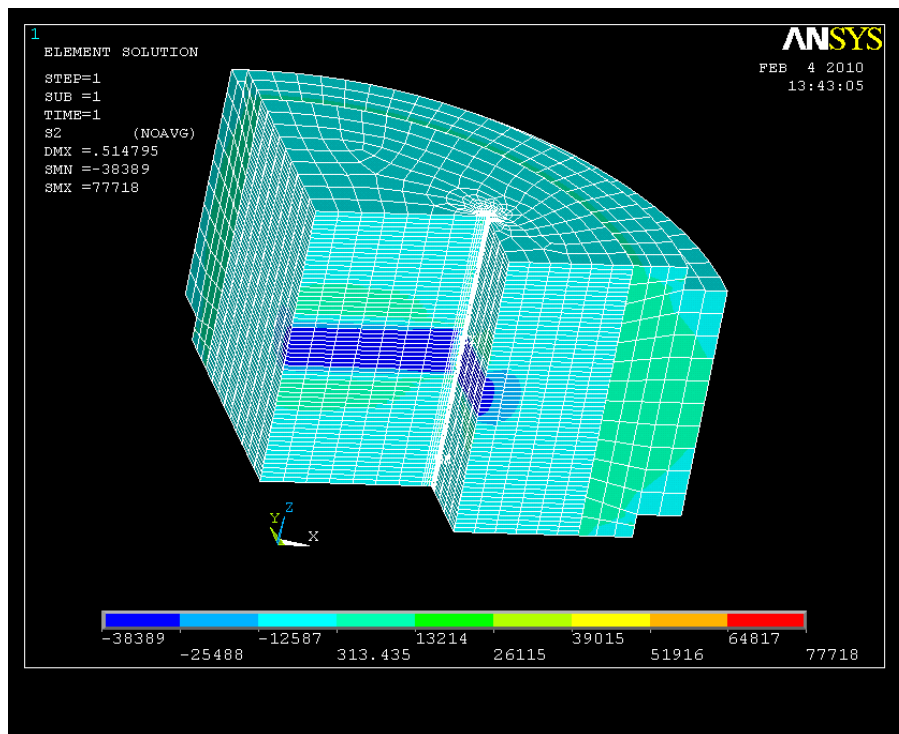


Fig. A.20. Second principal stress in europium oxide die with 0.004 in. interference fit.

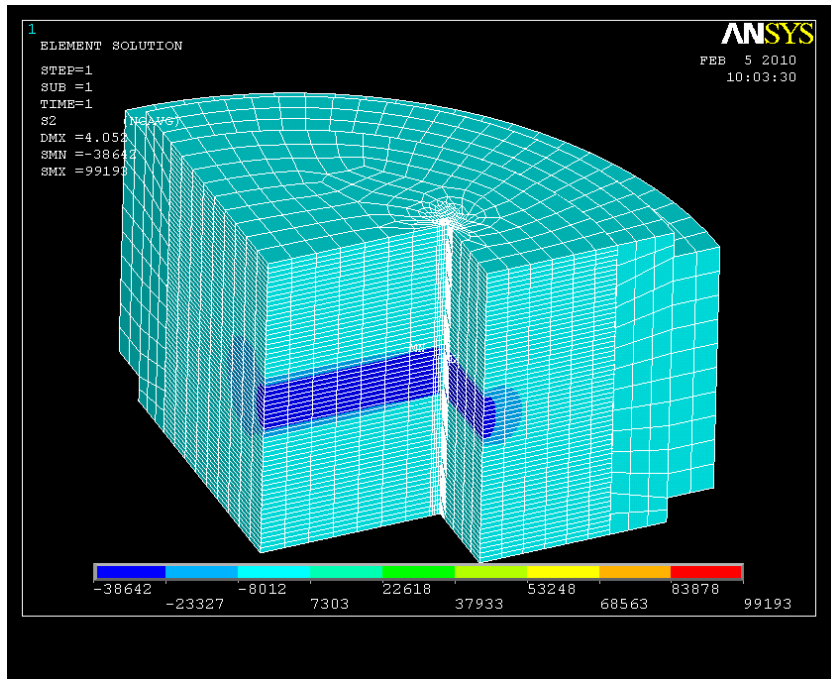


Fig. A.21. Second principal stress in europium oxide die with 0.003 in. interference fit.

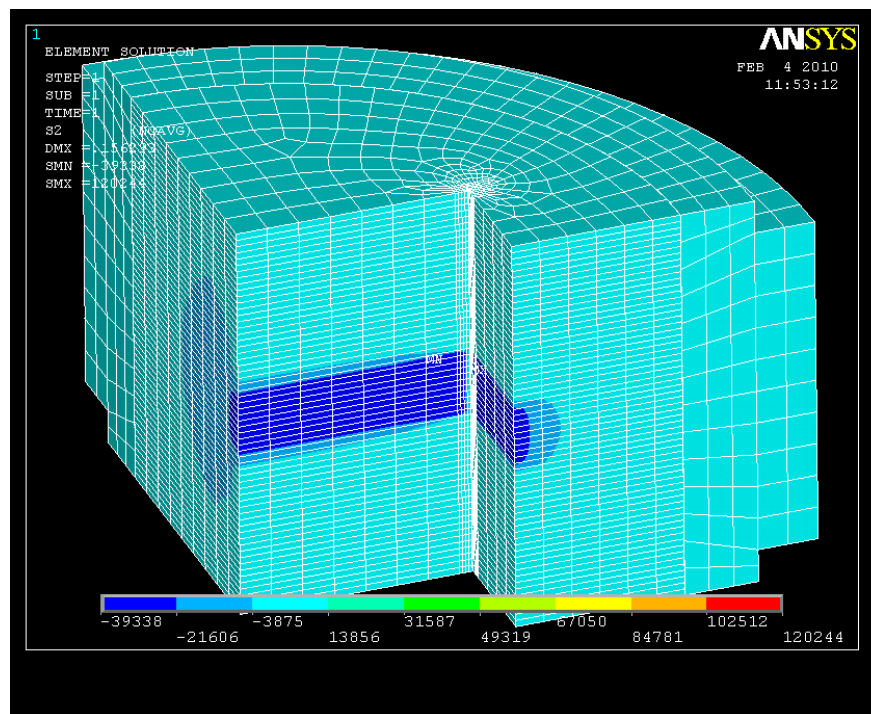


Fig. A.22. Second principal stress in europium oxide die with 0.002 in. interference fit.

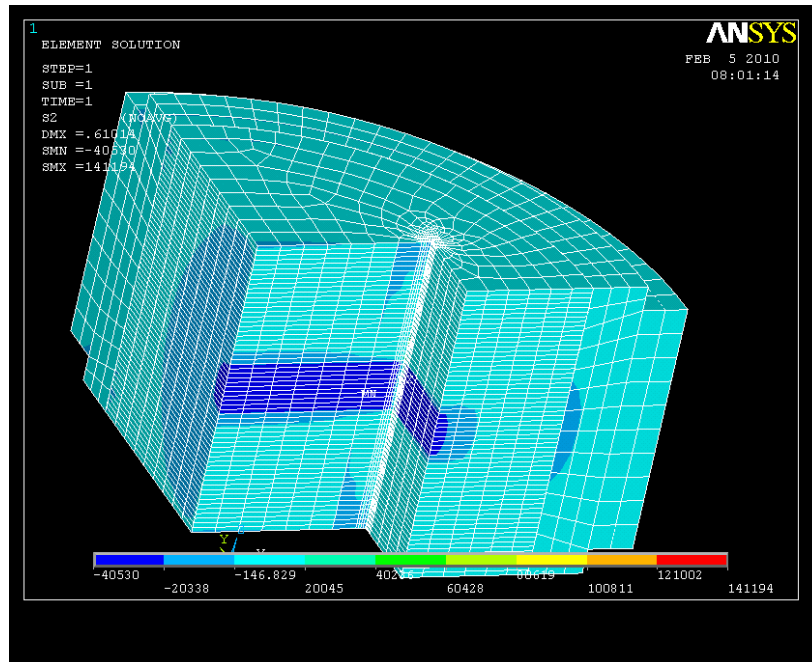


Fig. A.23. Second principal stress in europium oxide die with 0.001 in. interference fit.

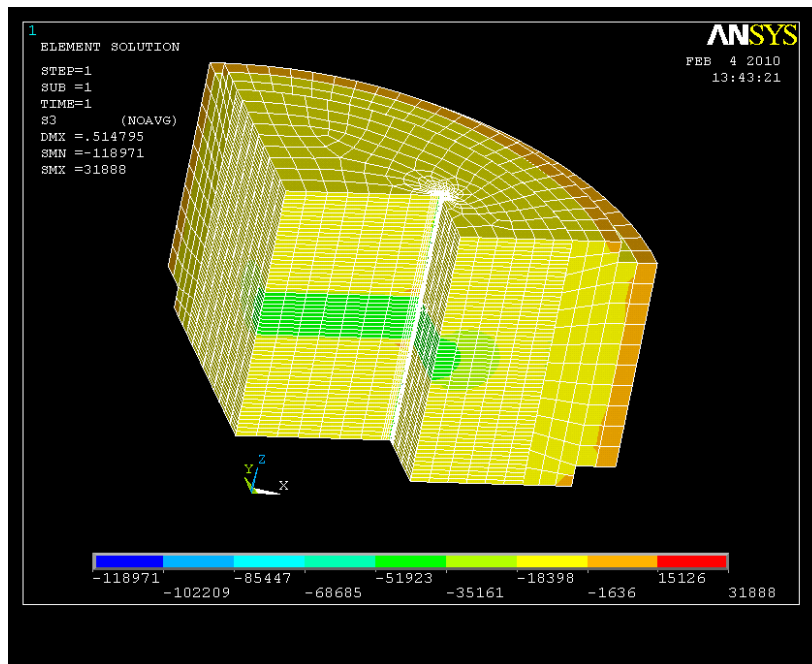


Fig. A.24. Third principal stress in europium oxide die with 0.004 in. interference fit.

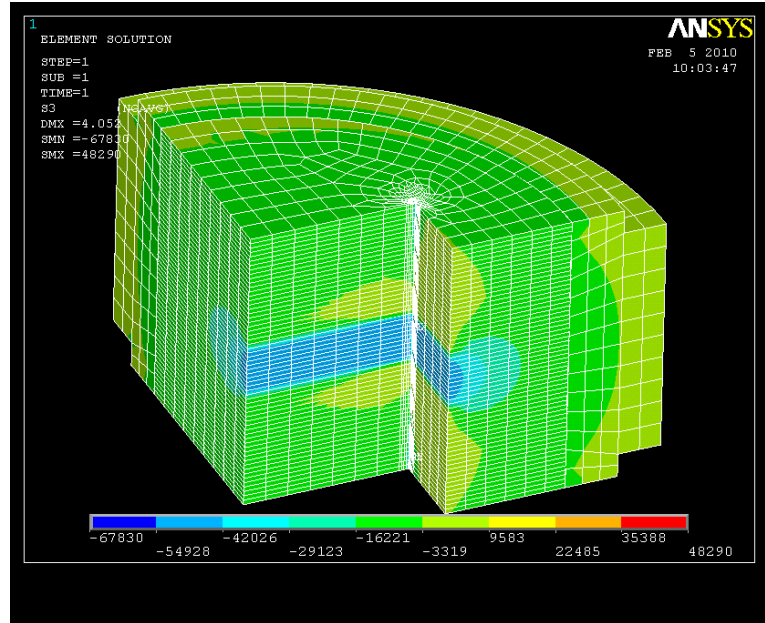


Fig. A.25. Third principal stress in europium oxide die with 0.003 in. interference fit.

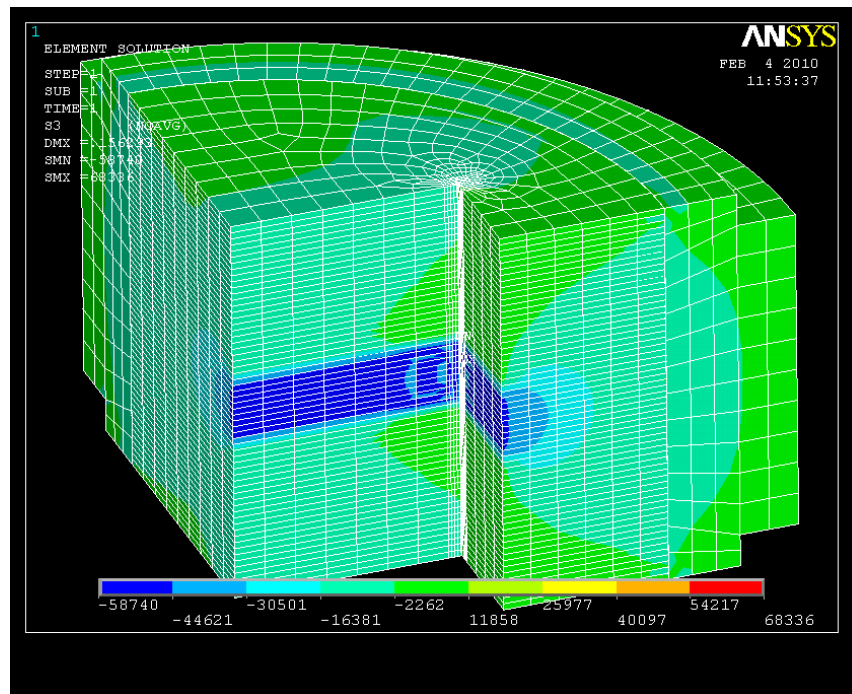


Fig. A.26. Third principal stress in europium oxide die with 0.002 in. interference fit.

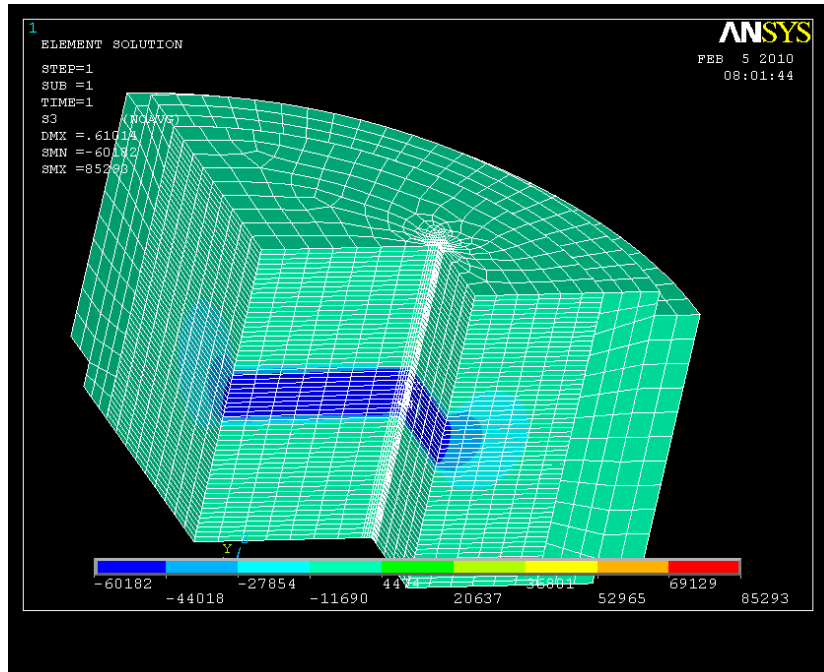


Fig. A.27. Third principal stress in europium oxide die with 0.001 in. interference fit.

The following stress contour plots show tantalum dies with the original geometry and in the no load (no compaction force) condition.

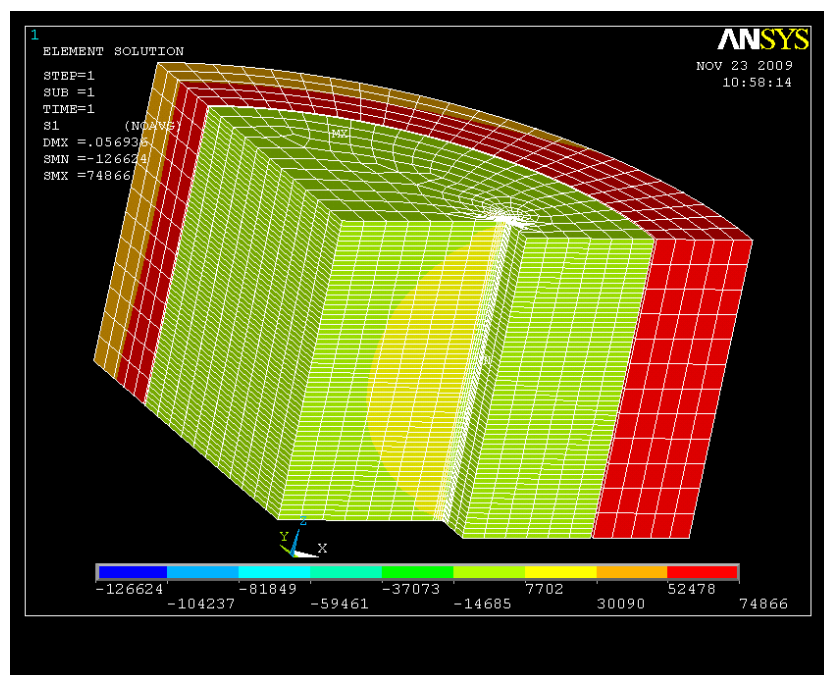


Fig. A.28. First principal stress in tantalum die with 0.01 in. interference fit.

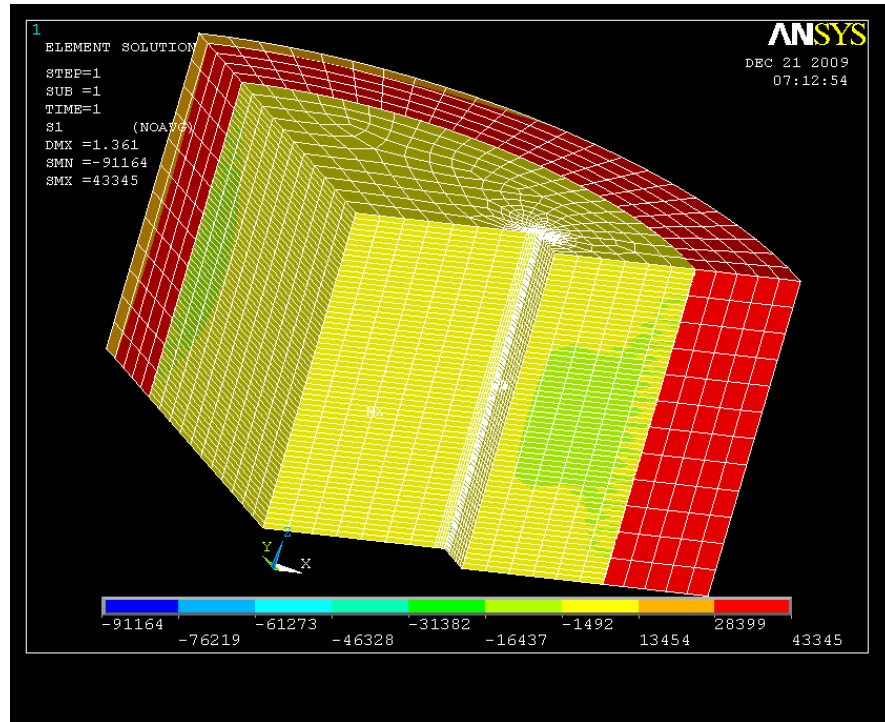


Fig. A.29. First principal stress in tantalum die with 0.006 in. interference fit.

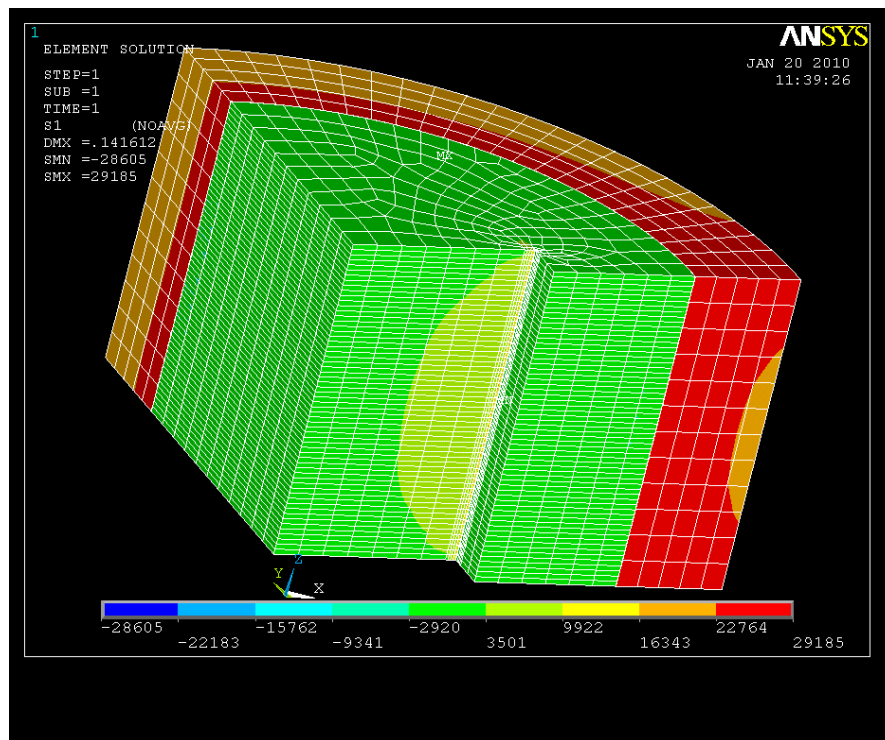


Fig. A.30. First principal stress in tantalum die with 0.004 in. interference fit.

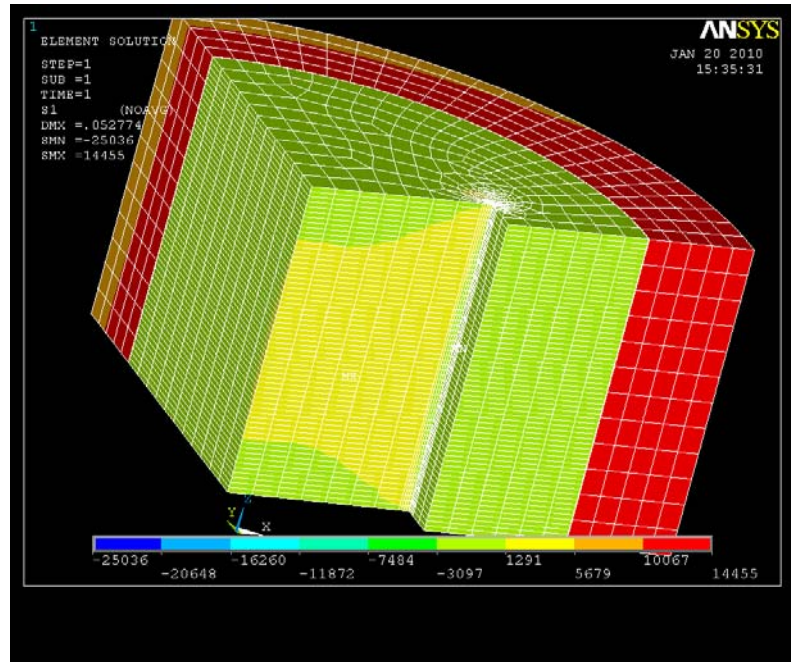


Fig. A.31. First principal stress in tantalum die with 0.002 in. interference fit.

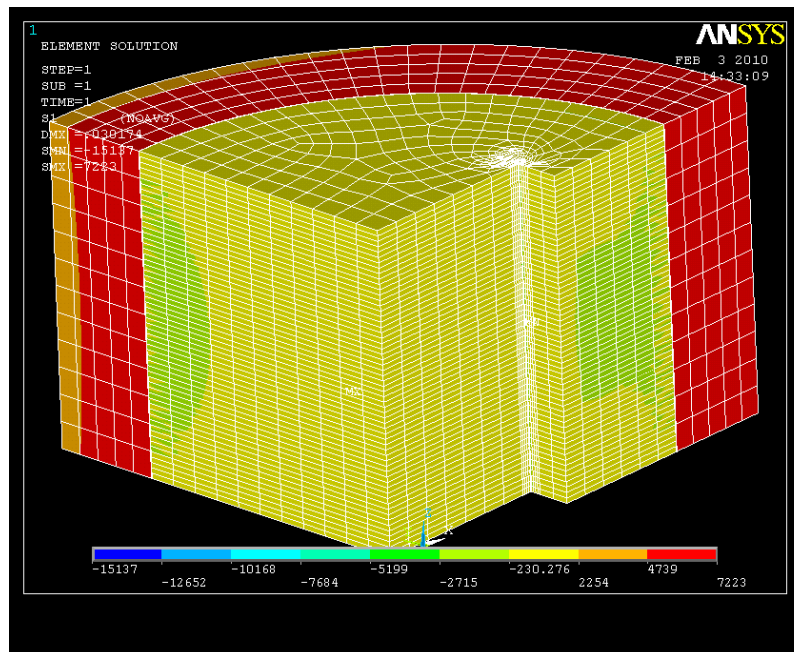


Fig. A.32. First principal stress in tantalum die with 0.001 in. interference fit.

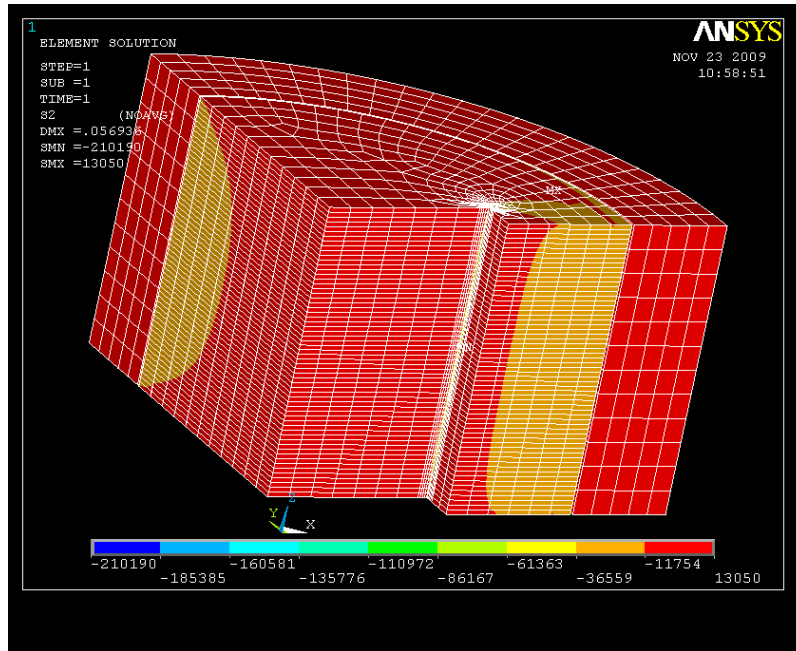


Fig. A.33. Second principal stress in tantalum die with 0.01 in. interference fit.

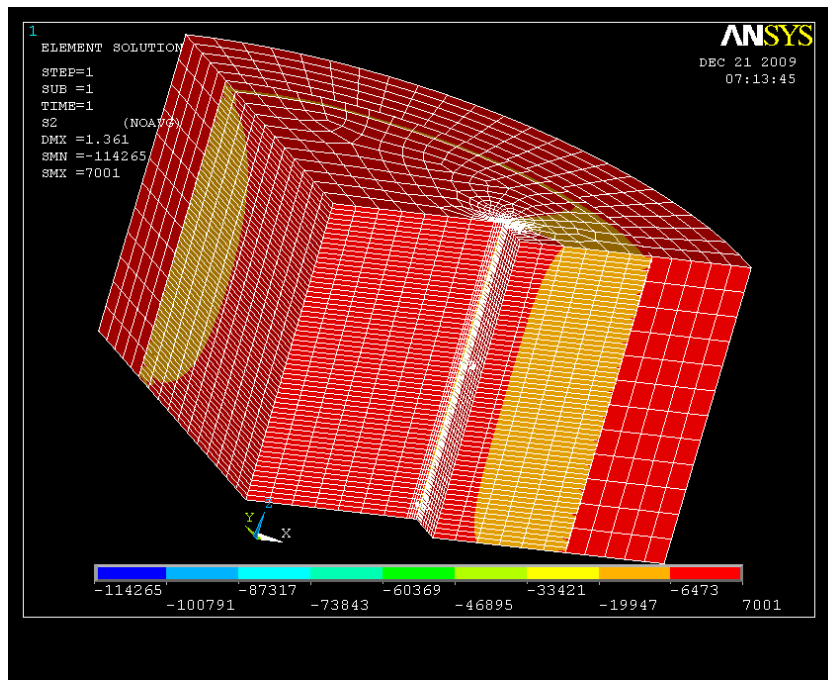


Fig. A.34. Second principal stress in tantalum die with 0.006 in. interference fit.

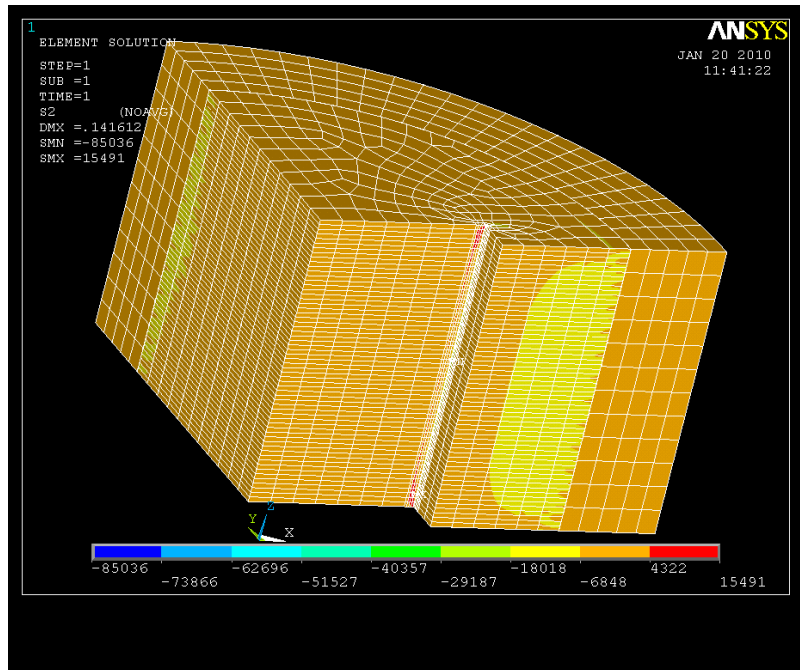


Fig. A.35. Second principal stress in tantalum die with 0.004 in. interference fit.

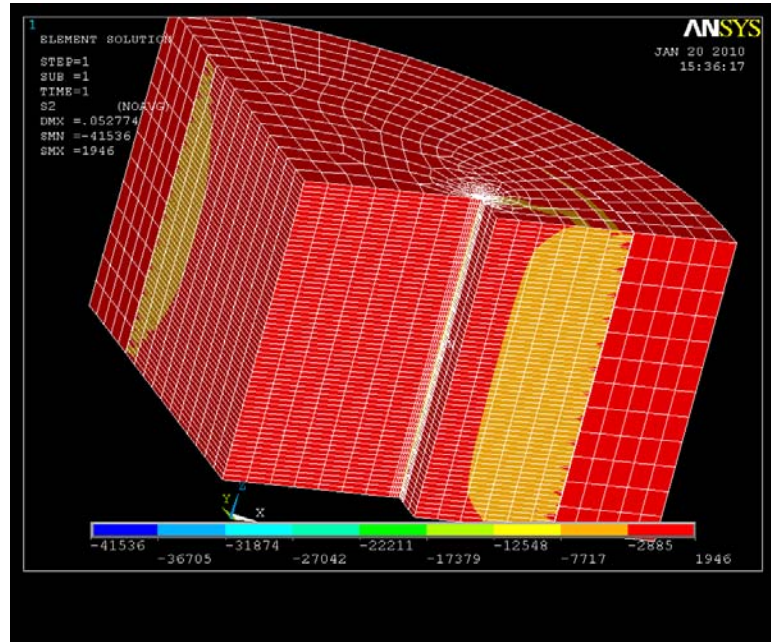


Fig. A.36. Second principal stress in tantalum die with 0.002 in. interference fit.

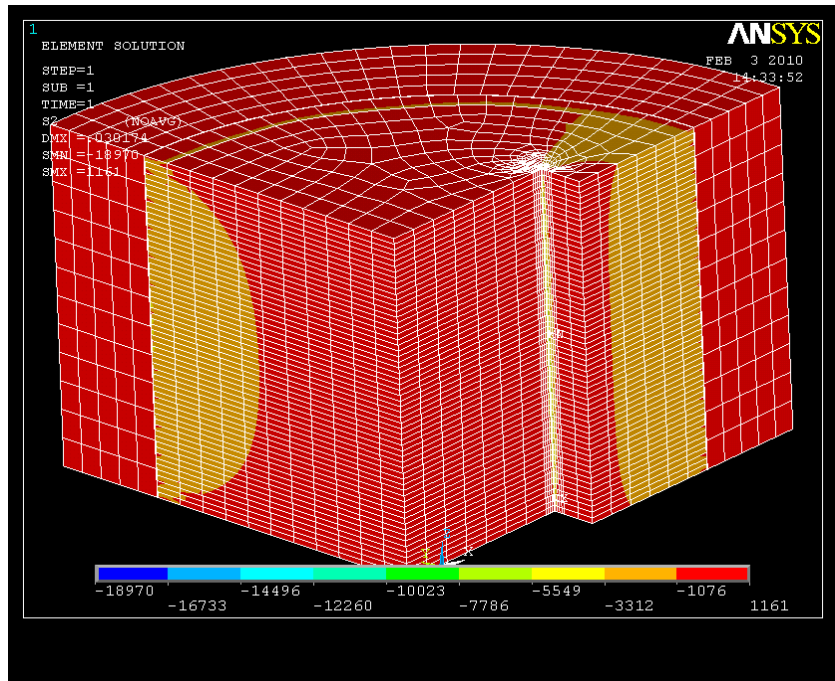


Fig. A.37. Second principal stress in tantalum die with 0.001 in. interference fit.

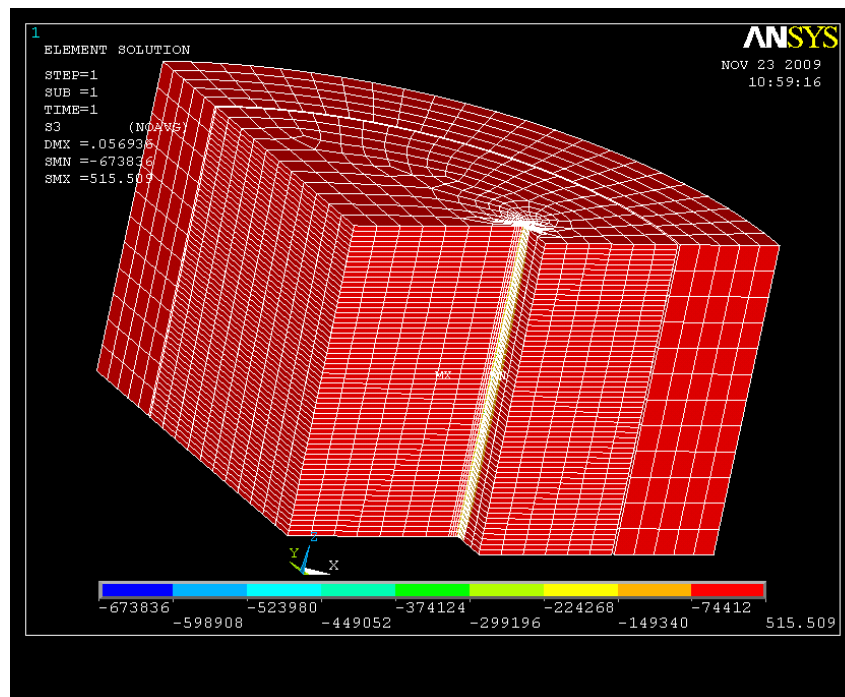


Fig. A.38. Third principal stress in tantalum die with 0.01 in. interference fit.

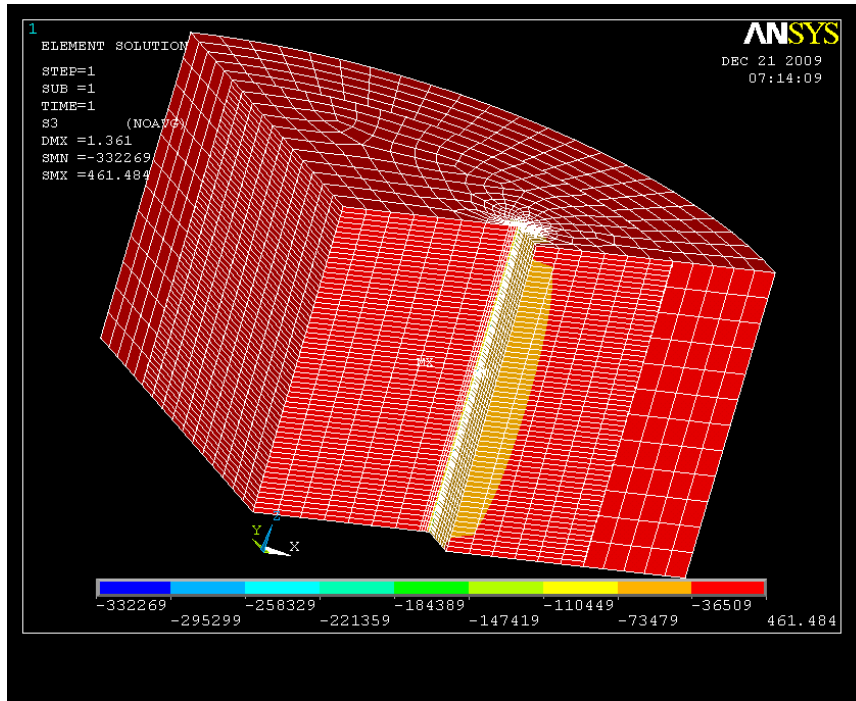


Fig. A.39. Third principal stress in tantalum die with 0.006 in. interference fit.

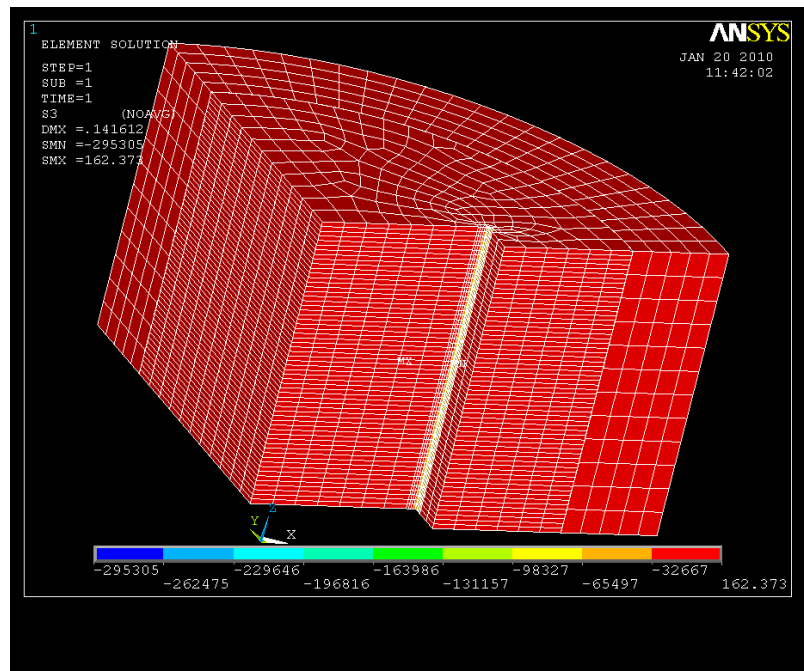


Fig. A.40. Third principal stress in tantalum die with 0.004 in. interference fit.

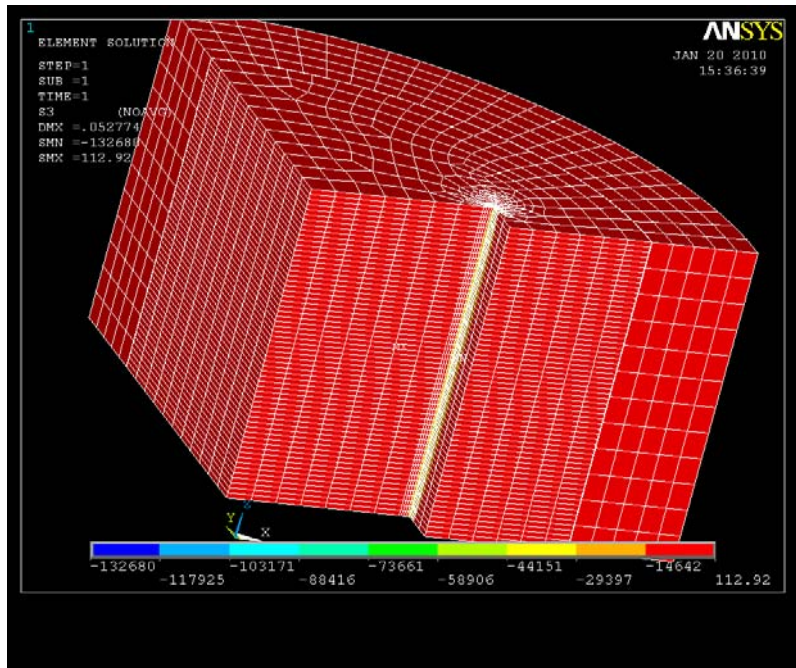


Fig. A.41. Third principal stress in tantalum die with 0.002 in. interference fit.

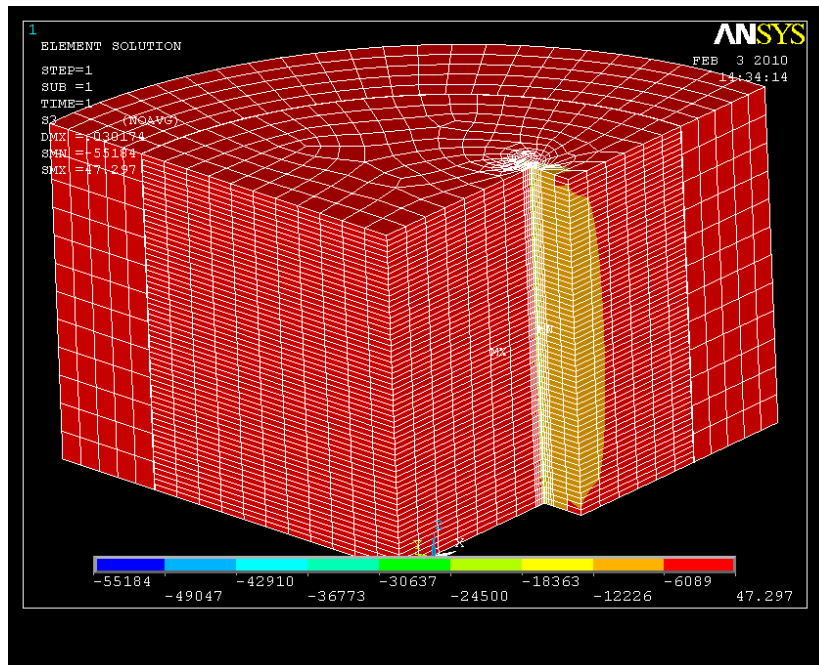


Fig. A.42. Third principal stress in tantalum die with 0.001 in. interference fit.

The following stress contour plots show tantalum dies with the original geometry and a 100,000 lb compaction force.

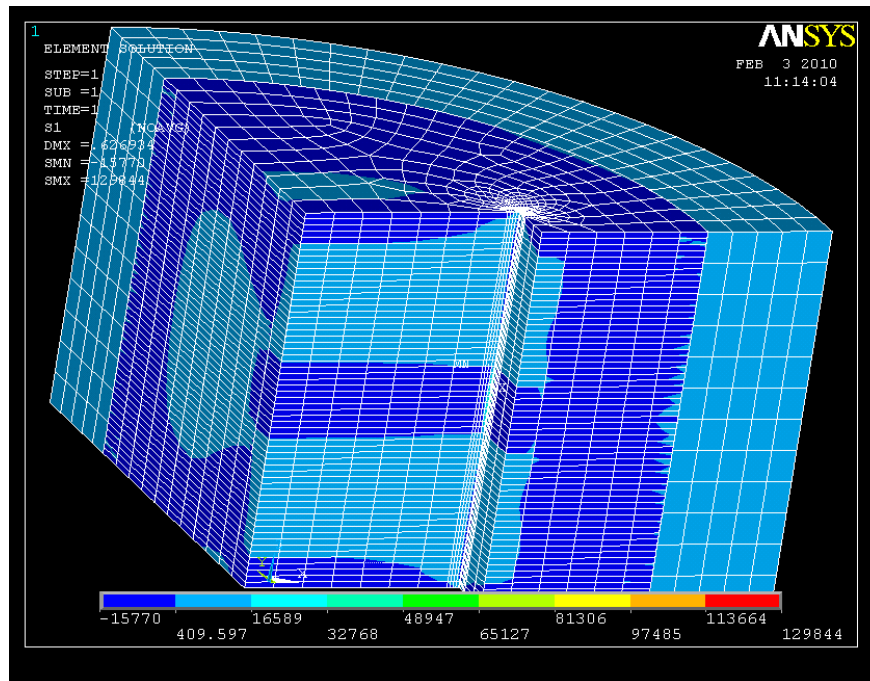


Fig. A.43. First principal stress in tantalum die with 0.002 in. interference fit.

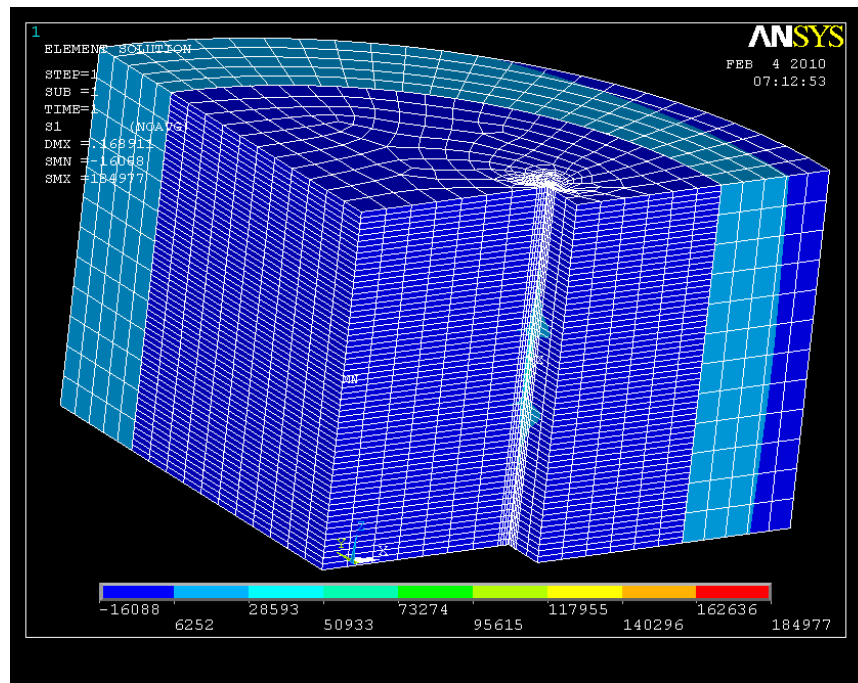


Fig. A.44. First principal stress in tantalum die with 0.001 in. interference fit.

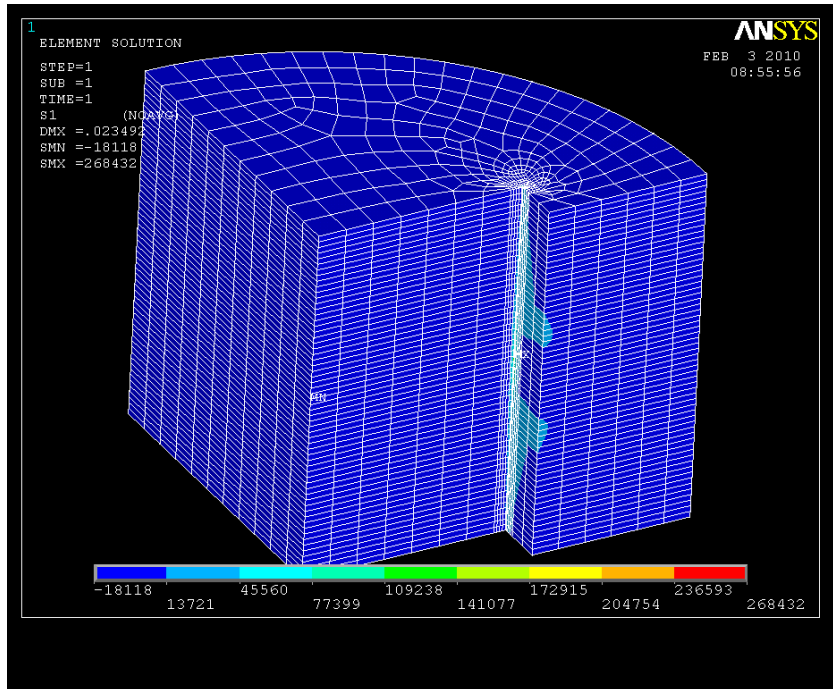


Fig. A.45. First principal stress in tantalum die with no interference fit.

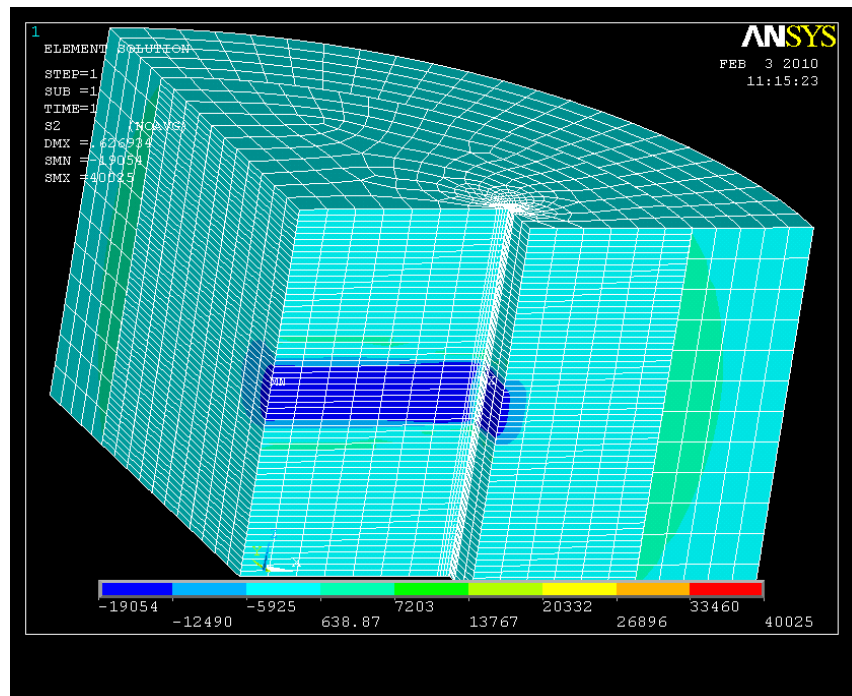


Fig. A.46. Second principal stress in tantalum die with 0.002 in. interference fit.

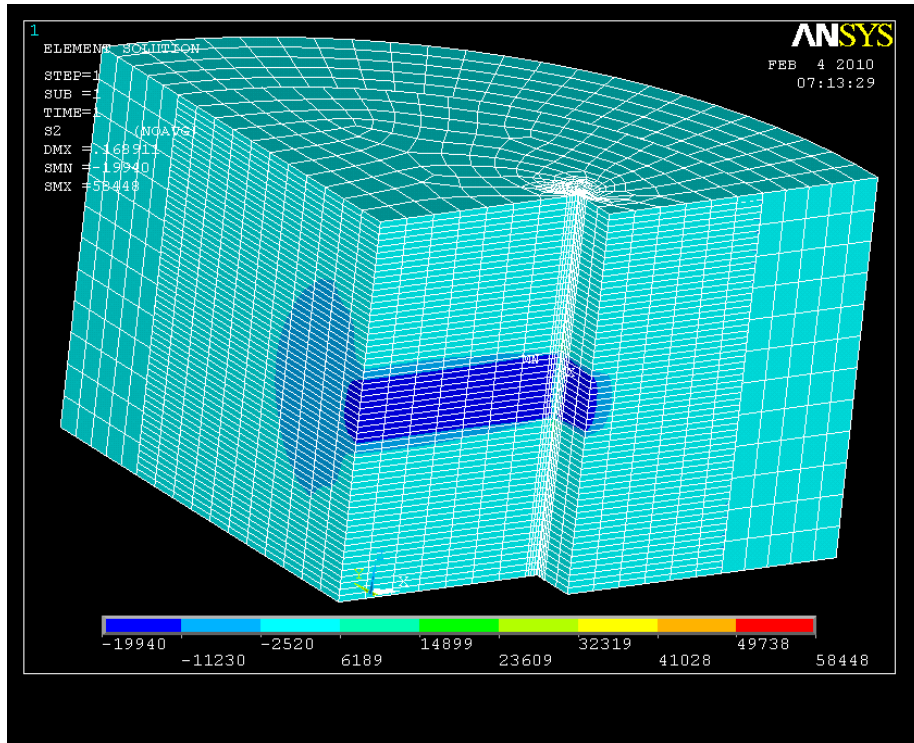


Fig. A.47. Second principal stress in tantalum die with 0.001 in. interference fit.

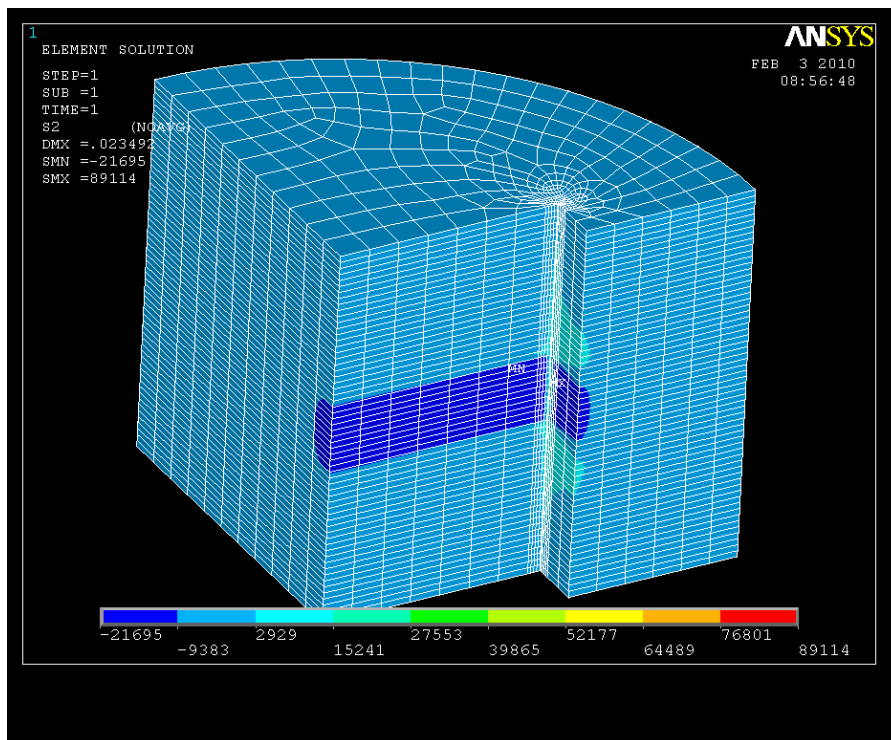


Fig. A.48. Second principal stress in tantalum die with no interference fit.

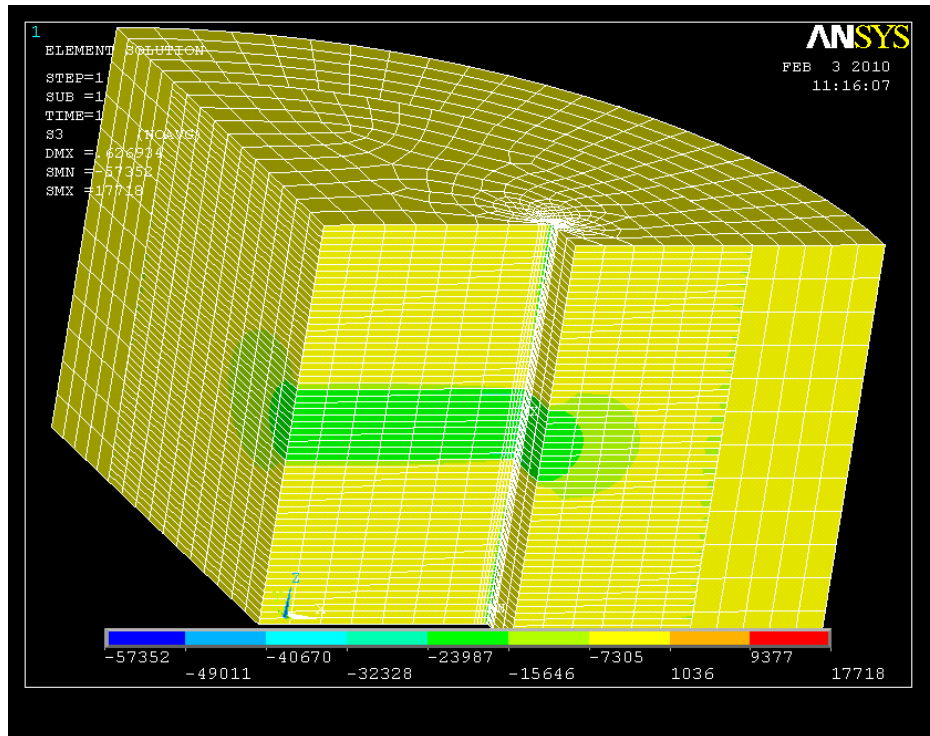


Fig. A.49. Third principal stress in tantalum die with 0.002 in. interference fit.

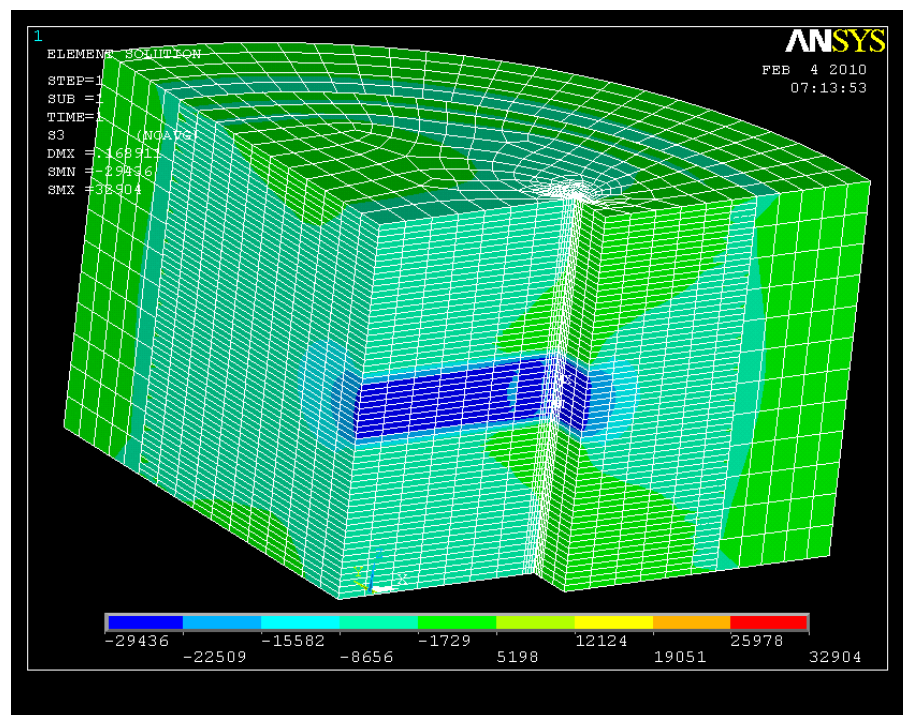


Fig. A.50. Third principal stress in tantalum die with 0.001 in. interference fit.

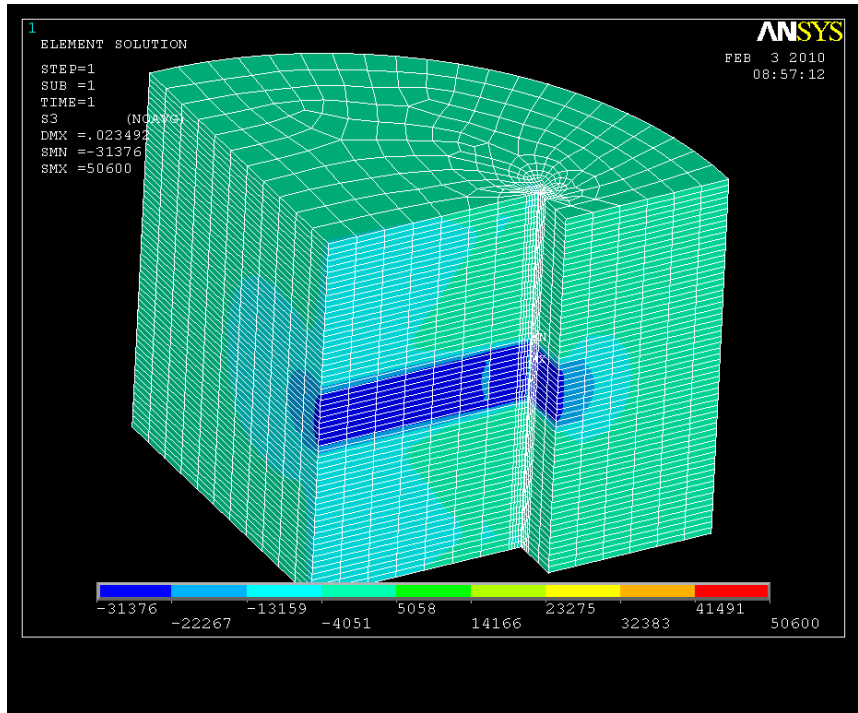


Fig. A.51. Third principal stress in tantalum die with no interference fit.

A.2 SMALLER WIRE DIAMETER

The following stress contour plots show europium oxide dies with a 0.003 in. interference fit and a 240,000 lb compaction force applied.

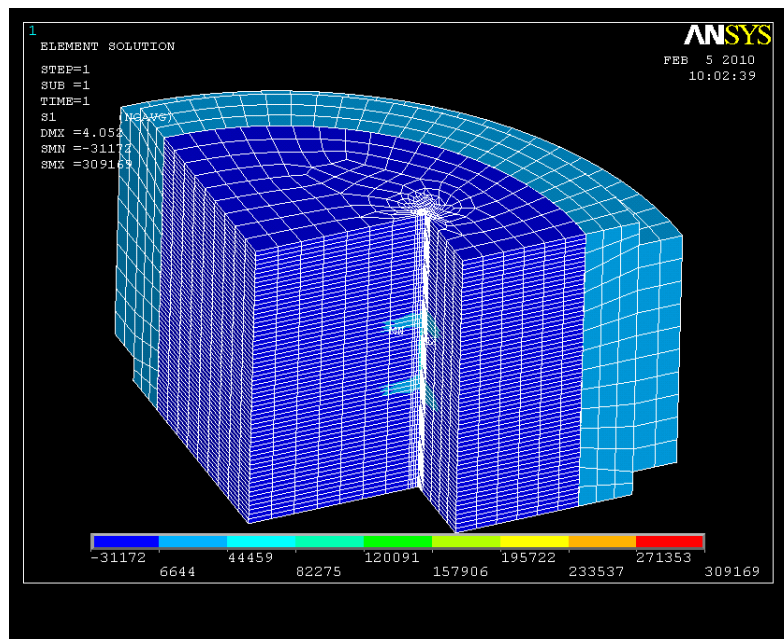


Fig. A.52. First principal stress in europium oxide die with 0.0055 in. inner corner radius.

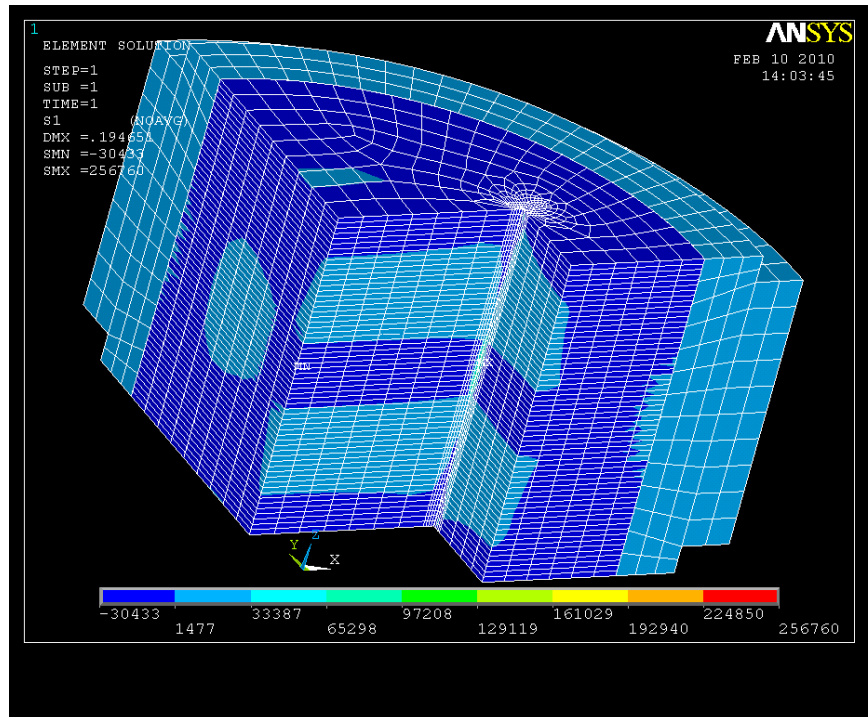


Fig. A.53. First principal stress in europium oxide die with 0.0030 in. inner corner radius.

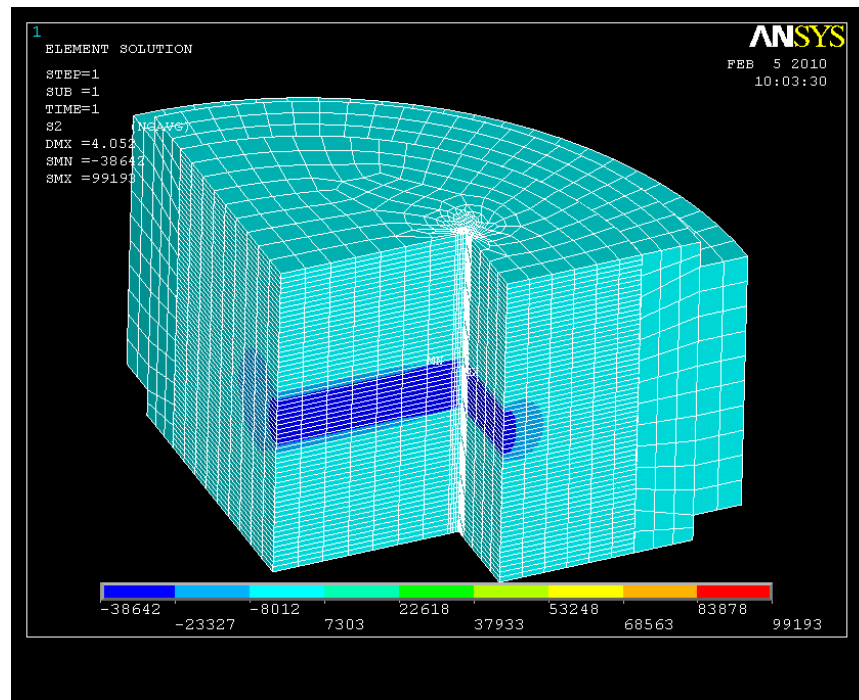


Fig. A.54. Second principal stress in europium oxide die with 0.0055 in. inner corner radius.

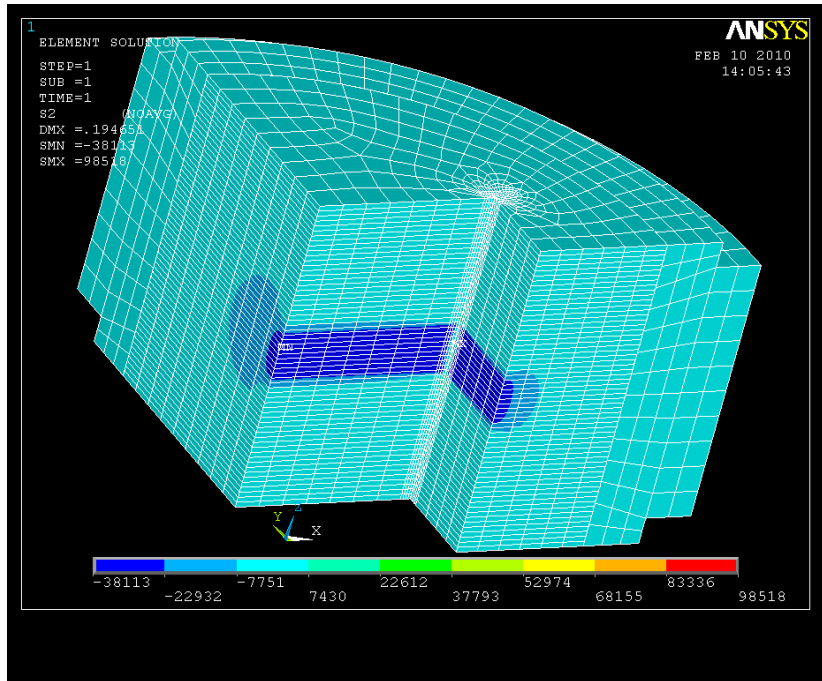


Fig. A.55. Second principal stress in europium oxide die with 0.0030 in. inner corner radius.

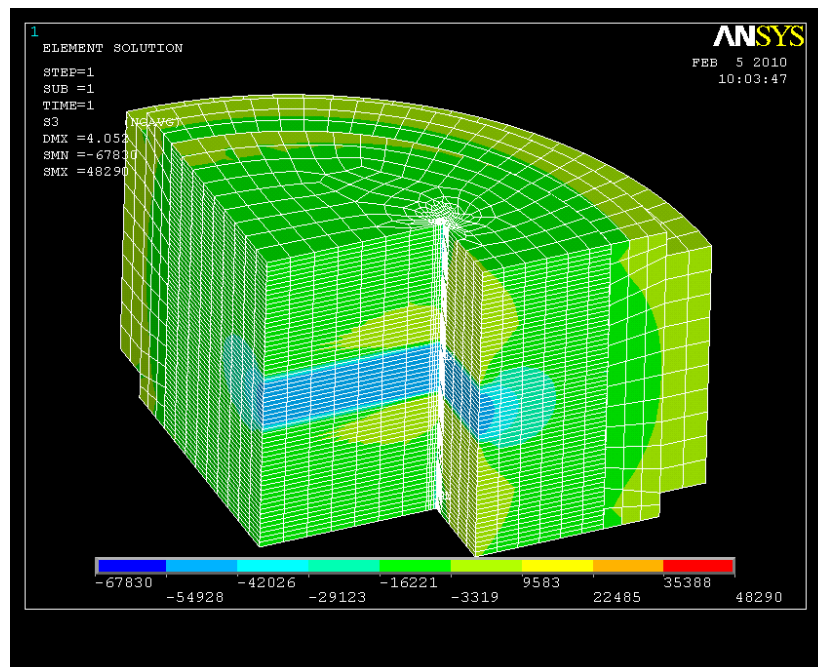


Fig. A.56. Third principal stress in europium oxide die with 0.0055 in. inner corner radius.

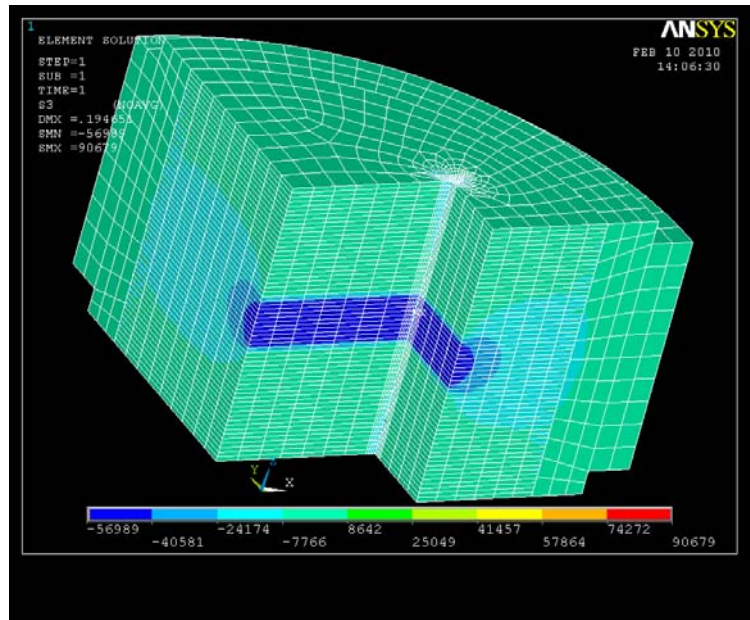


Fig. A.57. Third principal stress in europium oxide die with 0.0030 in. inner corner radius.

A.3 SMALLER COMPACTION FORCE

The following stress contour plots show europium oxide dies with a 0.003 in. interference fit.

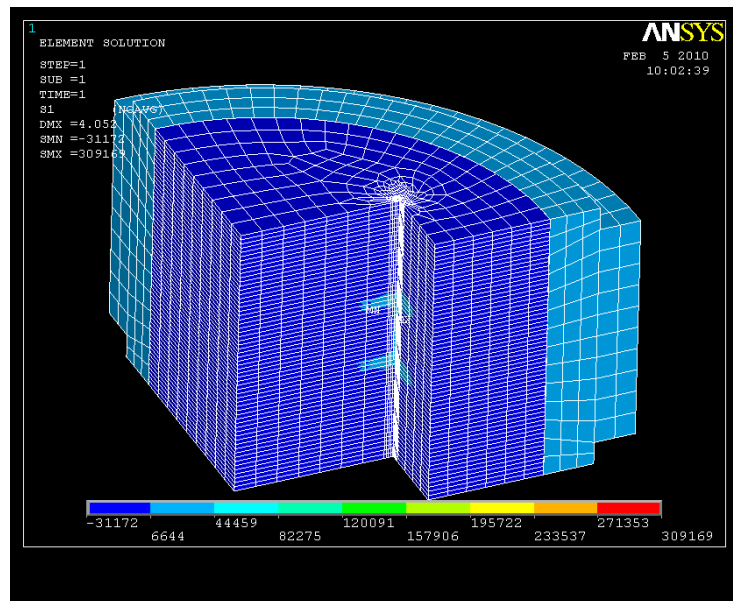


Fig. A.58. First principal stress in europium oxide die with 240,000 lb applied.

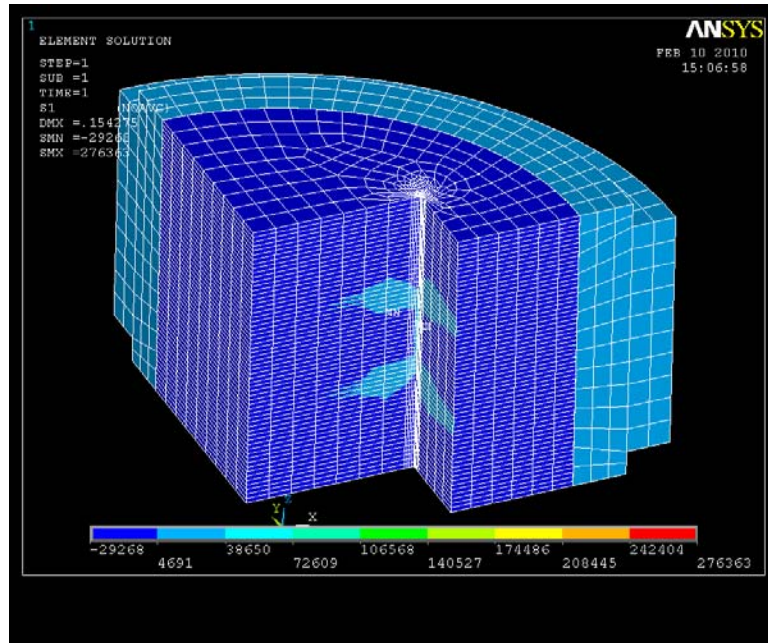


Fig. A.59. First principal stress in europium oxide die with 224,000 lb applied.

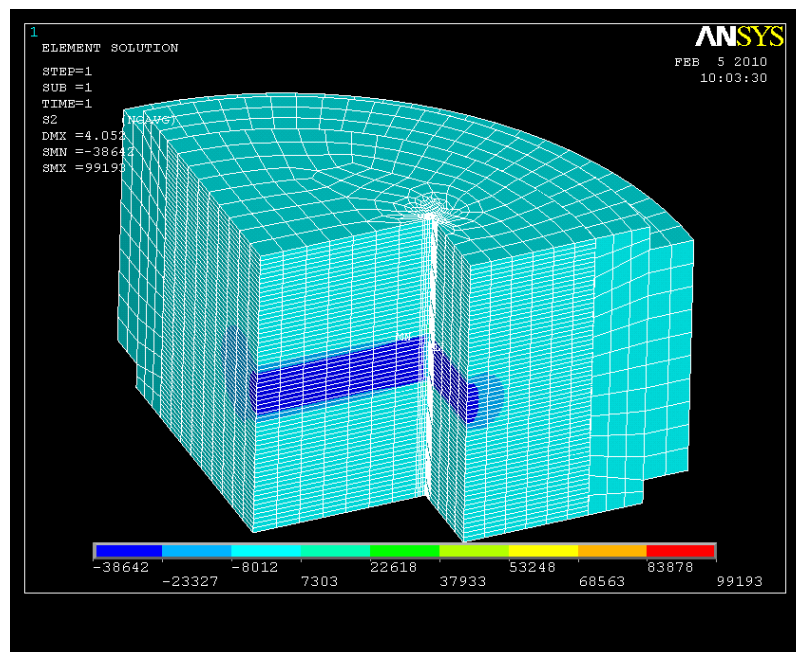


Fig. A.60. Second principal stress in europium oxide die with 240,000 lb applied.

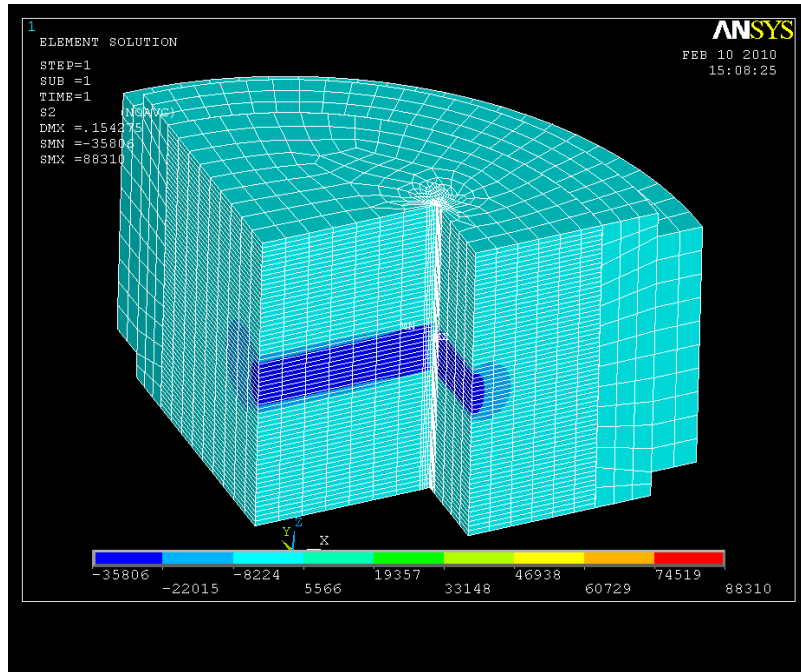


Fig. A.61. Second principal stress in europium oxide die with 224,000 lb applied.

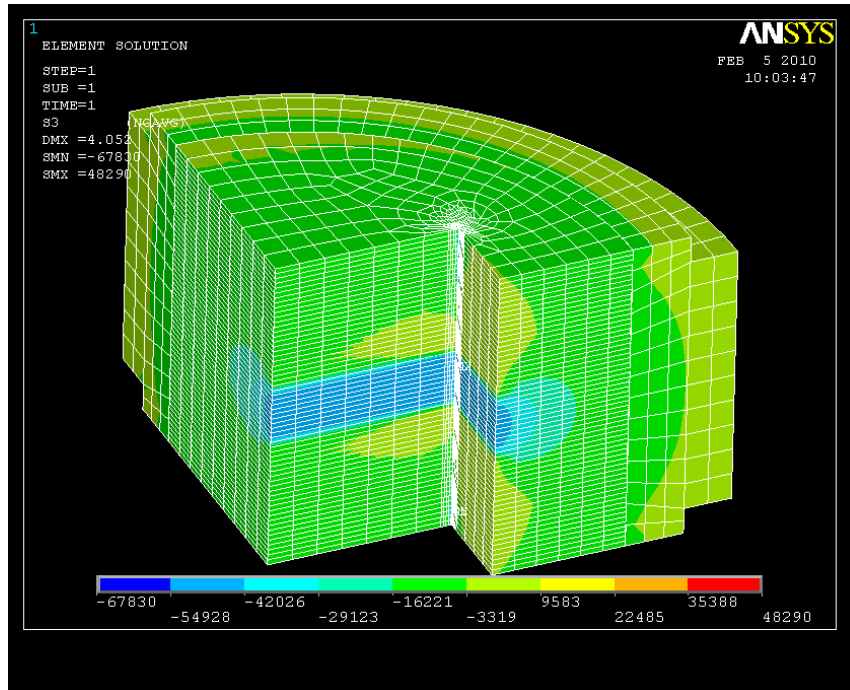


Fig. A.62. Third principal stress in europium oxide die with 240,000 lb applied.

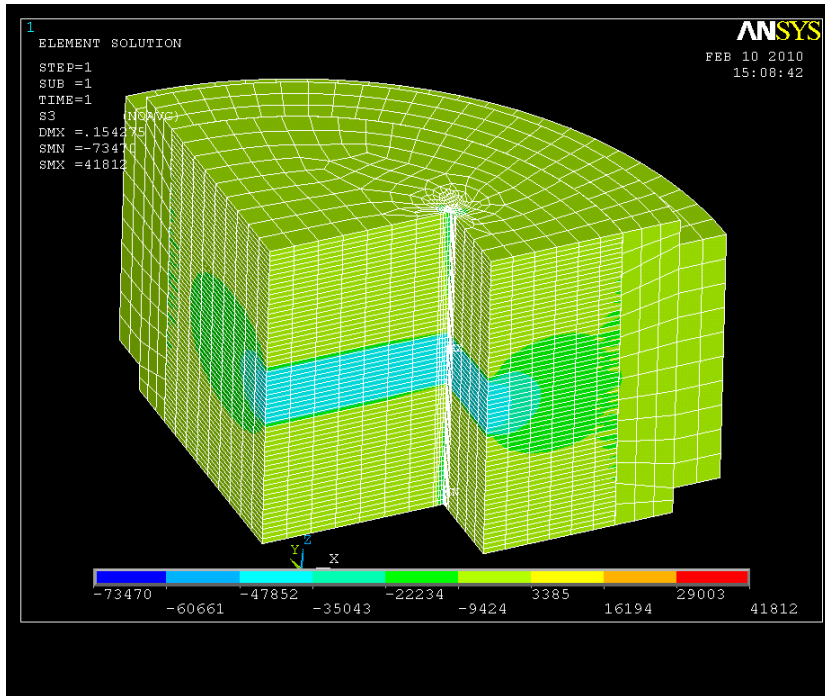


Fig. A.63. Third principal stress in europium oxide die with 224,000 lb applied.

The following stress contour plots show tantalum dies with a 0.001 in. interference fit.

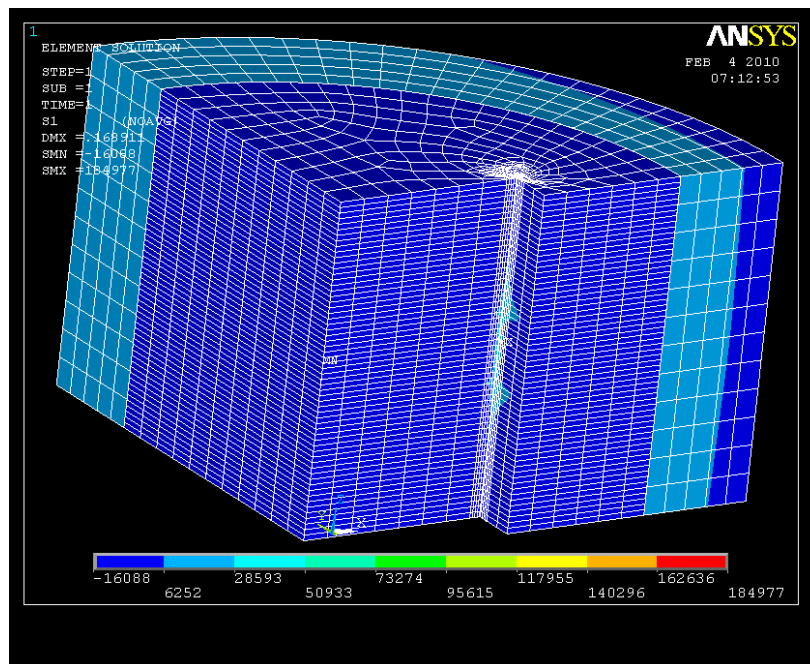


Fig. A.64. First principal stress in tantalum die with 100,000 lb applied.

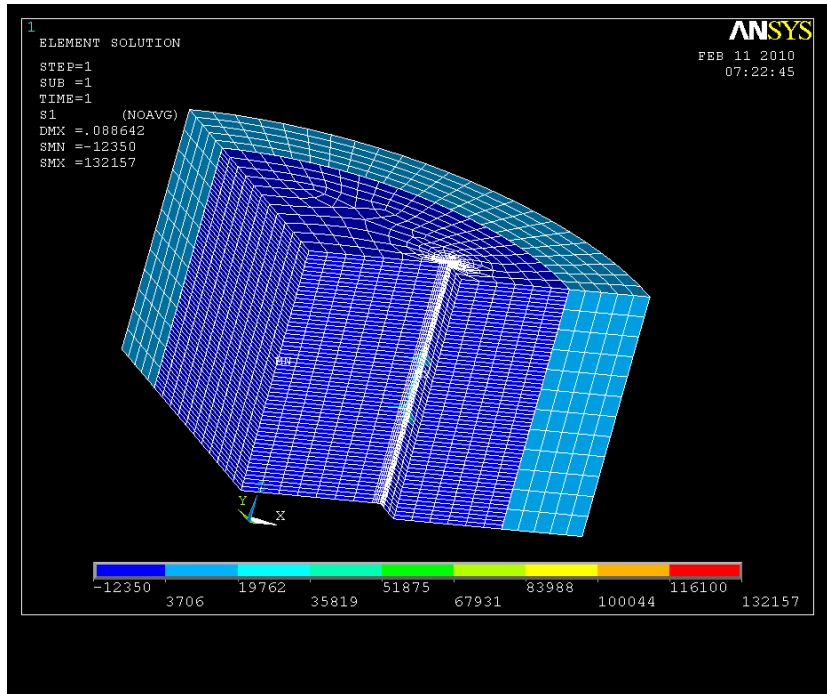


Fig. A.65. First principal stress in tantalum die with 78,000 lb applied.

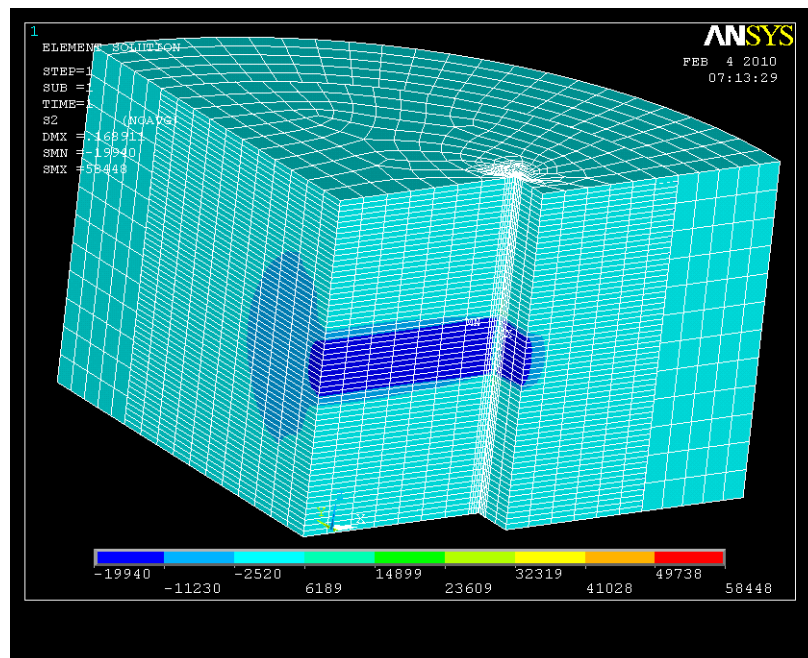


Fig. A.66. Second principal stress in tantalum die with 100,000 lb applied.

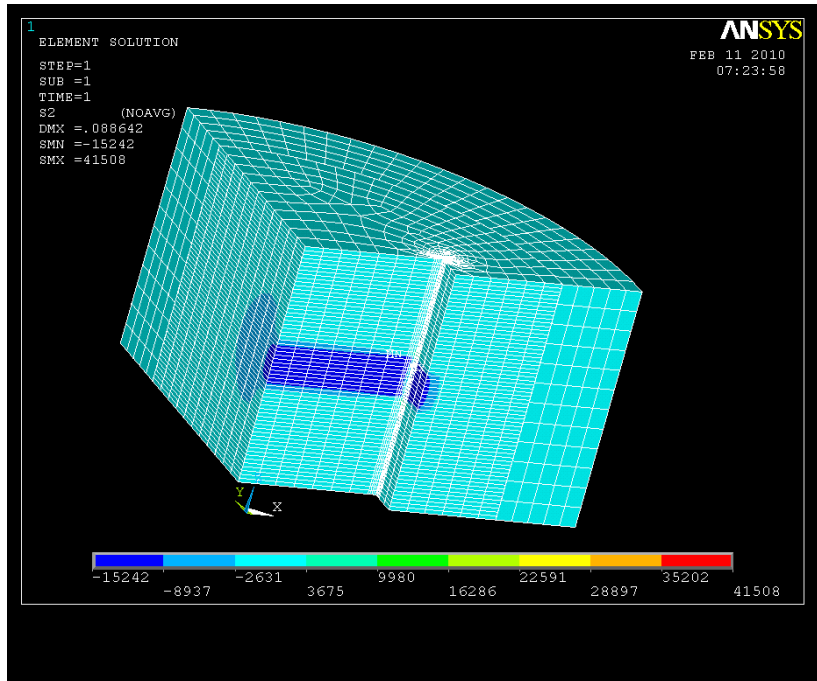


Fig. A.67. Second principal stress in tantalum die with 78,000 lb applied.

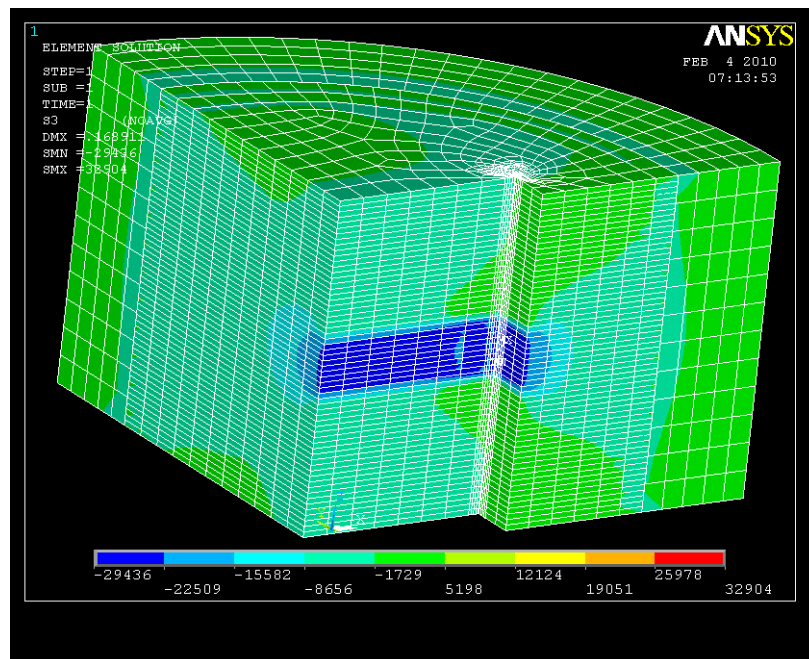


Fig. A.68. Third principal stress in tantalum die with 100,000 lb applied.

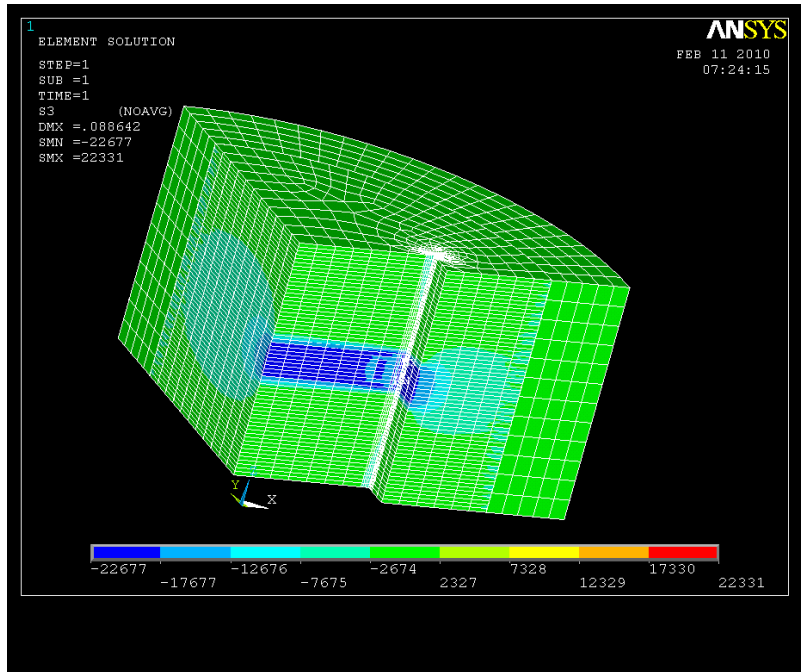


Fig. A.69. Third principal stress in tantalum die with 78,000 lb applied.

A.4 LARGER INNER CAVITY

The following stress contour plots show europium oxide dies with a 0.003 in. interference fit and in the loaded condition with a 240,000 lb compaction force.

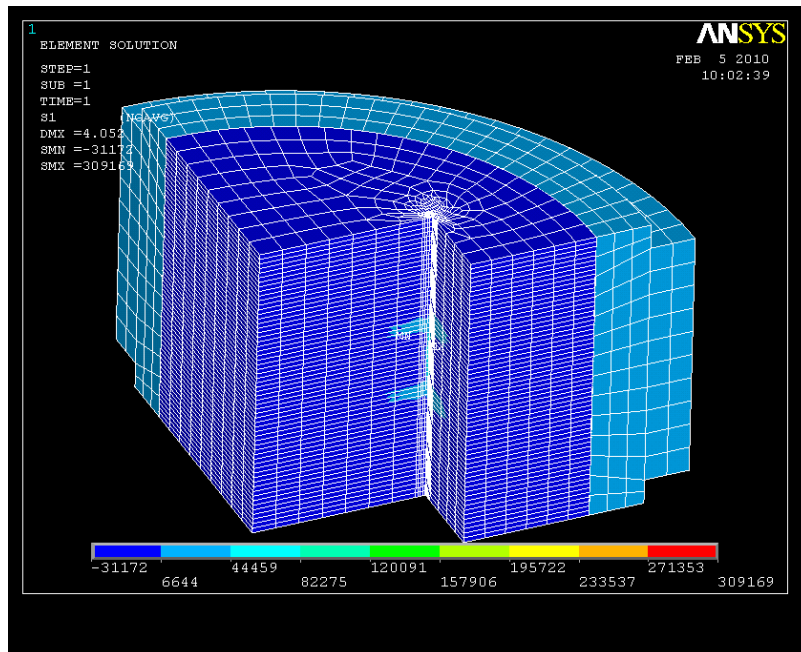


Fig. A.70. First principal stress in europium oxide die with original geometry.

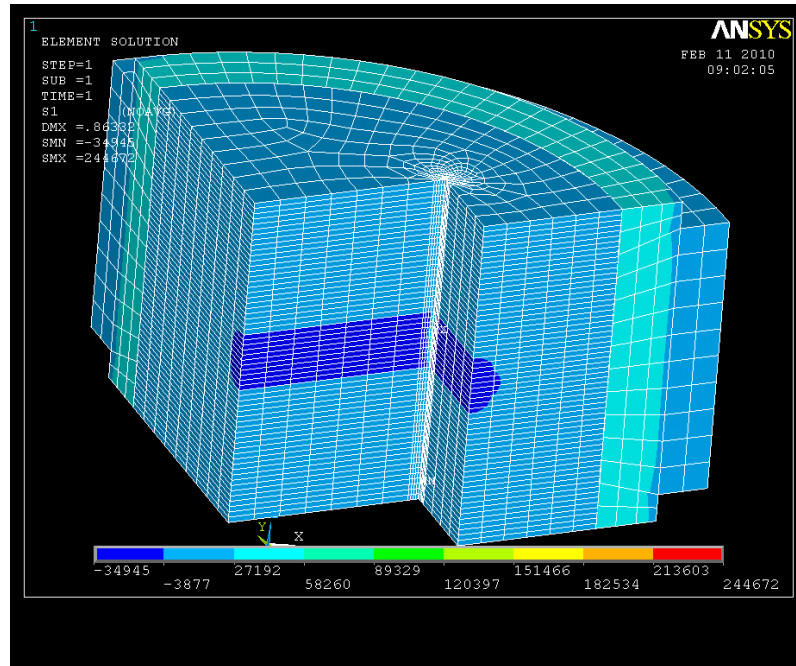


Fig. A.71. First principal stress in europium oxide die with cavity size increased by 0.002 in. per side.

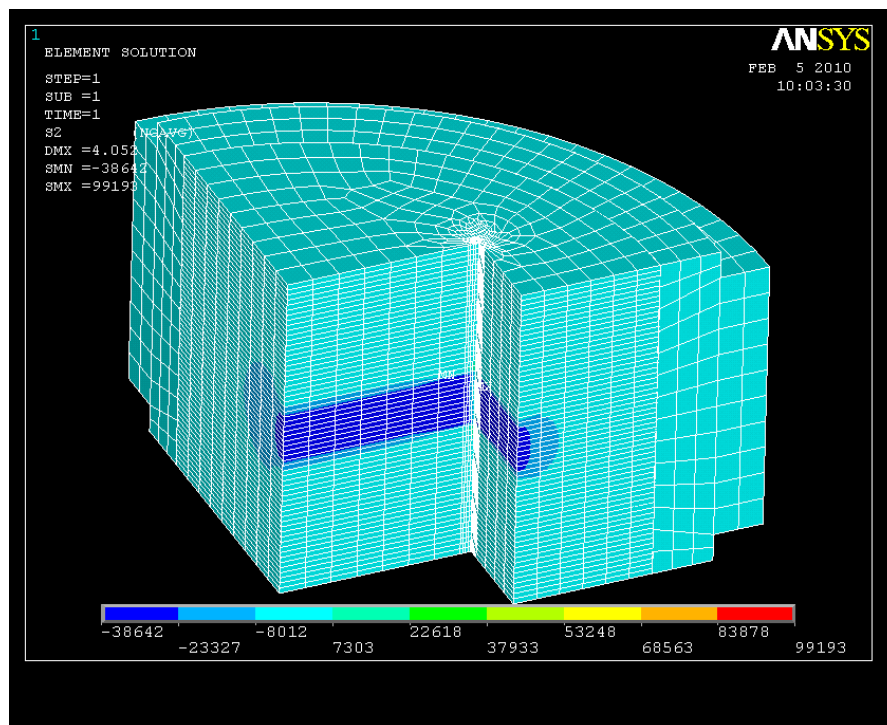


Fig. A.72. Second principal stress in europium oxide die with original geometry.

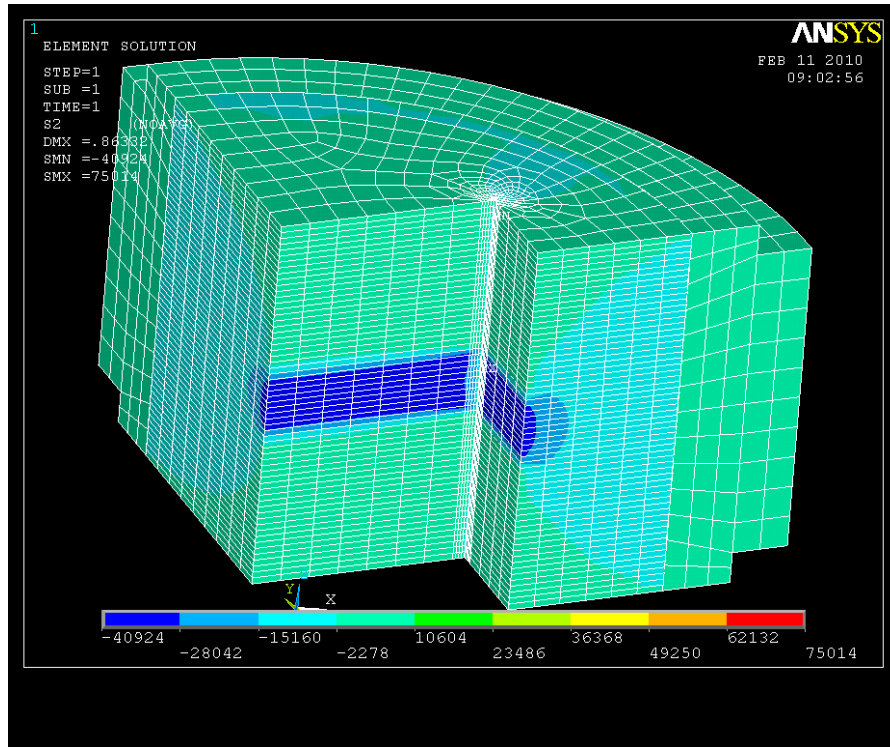


Fig. A.73. Second principal stress in europium oxide die with cavity size increased by 0.002 in. per side.

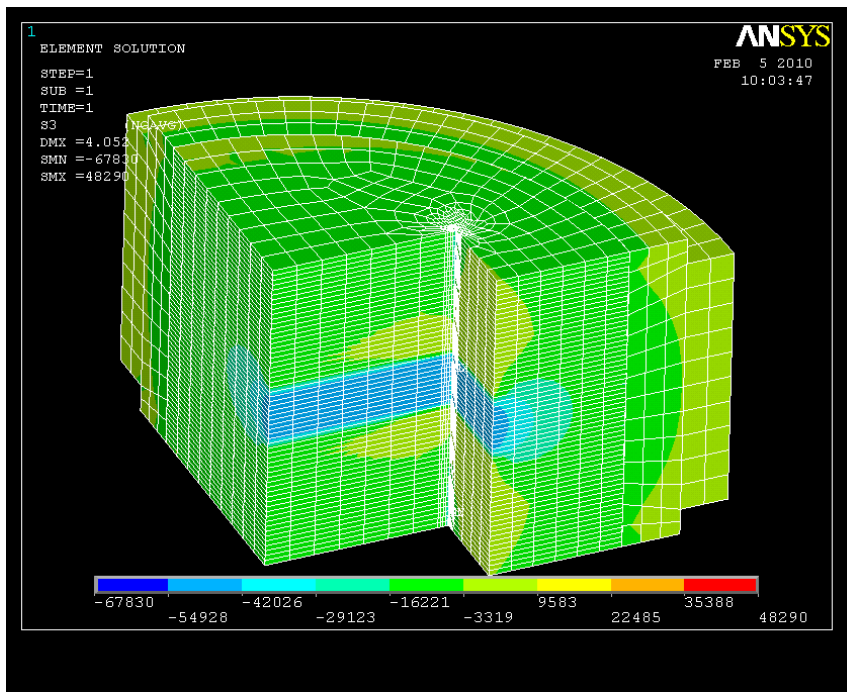


Fig. A.74. Third principal stress in europium oxide die with original geometry.

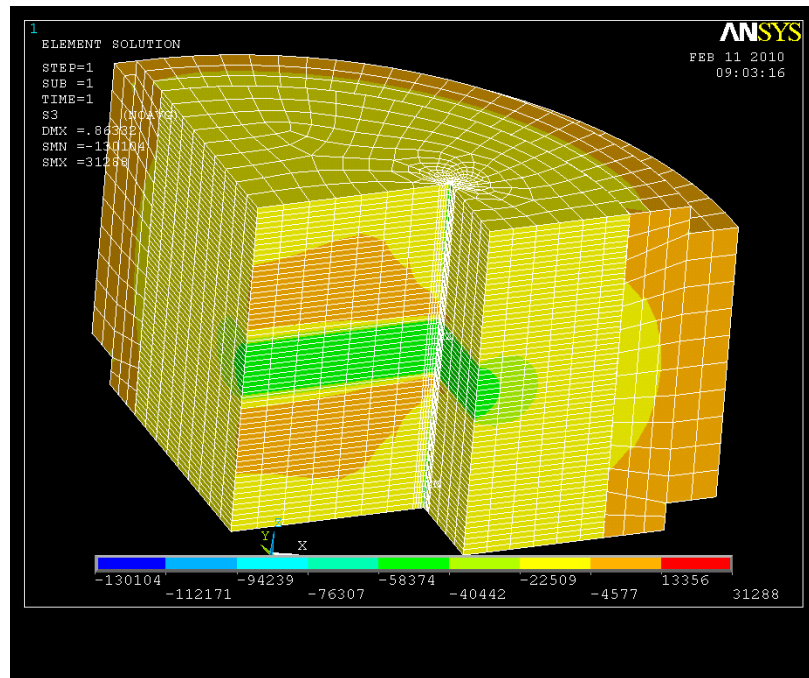


Fig. A.75. Third principal stress in europium oxide die with cavity size increased by 0.002 in. per side.

A.4 LARGER OUTER RADIUS

The following stress contour plots show europium oxide dies with a 0.003 in. interference fit and a compaction force of 240,000 lb.

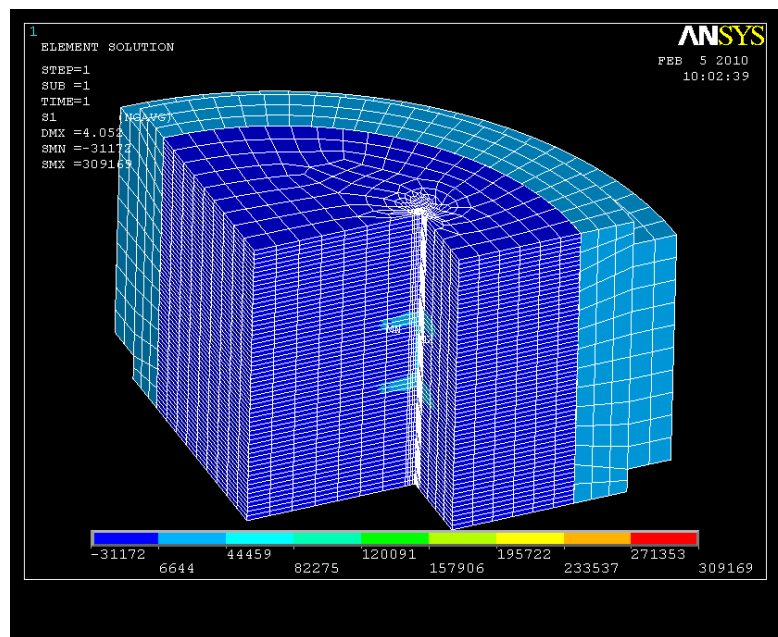


Fig. A.76. First principal stress in europium oxide die with original geometry.

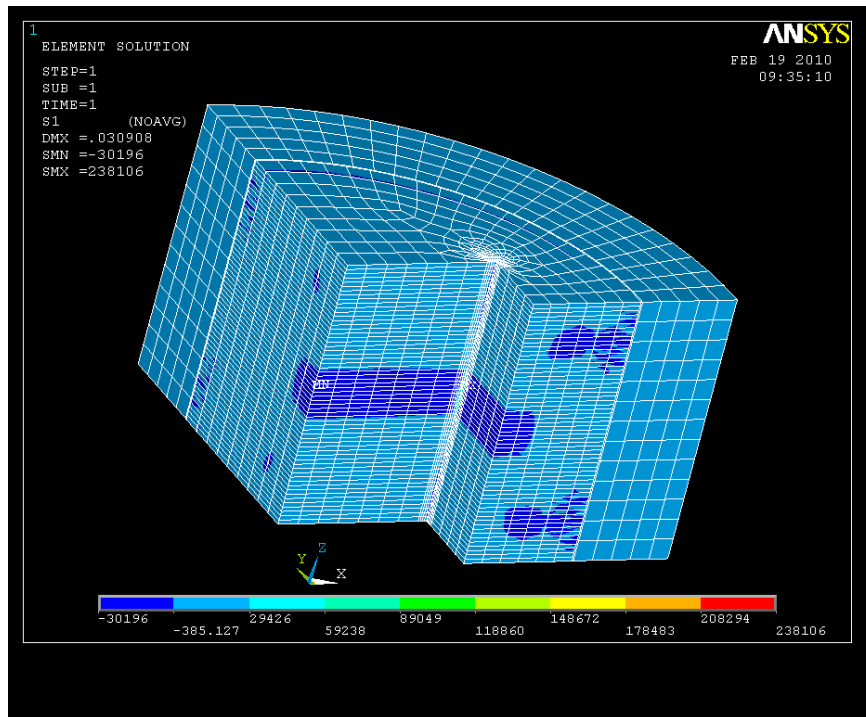


Fig. A.77. First principal stress in europium oxide die with tantalum die's outer radius geometry.

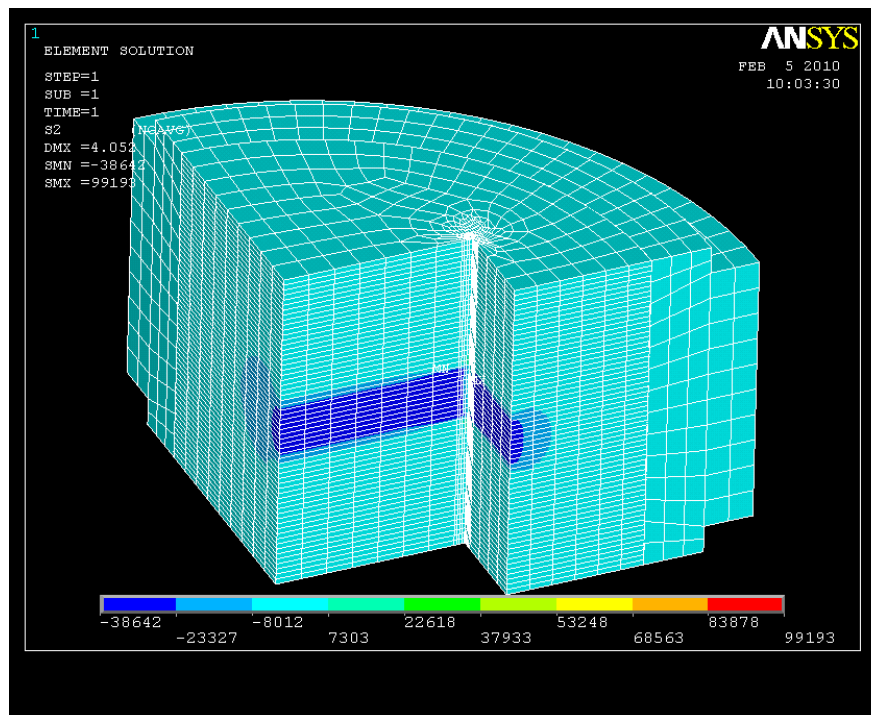


Fig. A.78. Second principal stress in europium oxide die with original geometry.

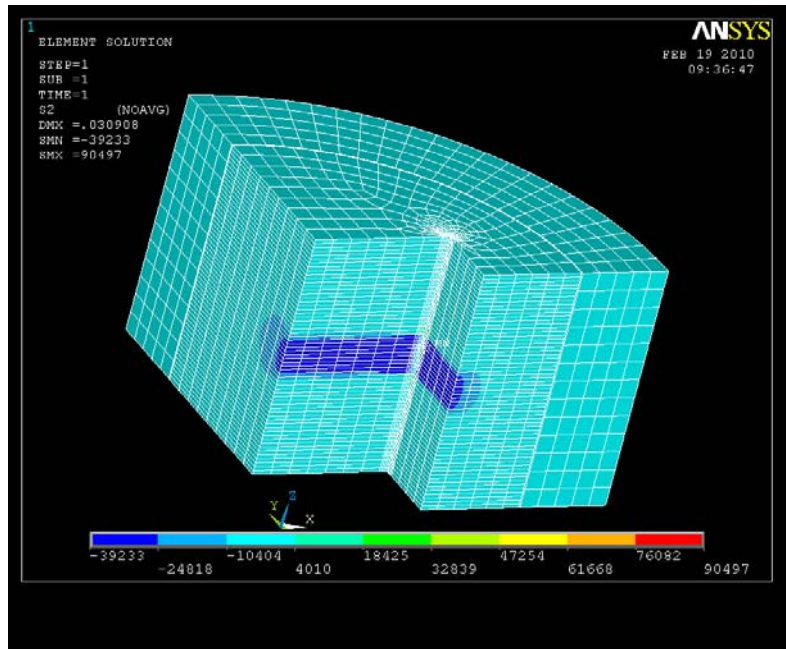


Fig. A.79. Second principal stress in europium oxide die with tantalum die's outer radius geometry.

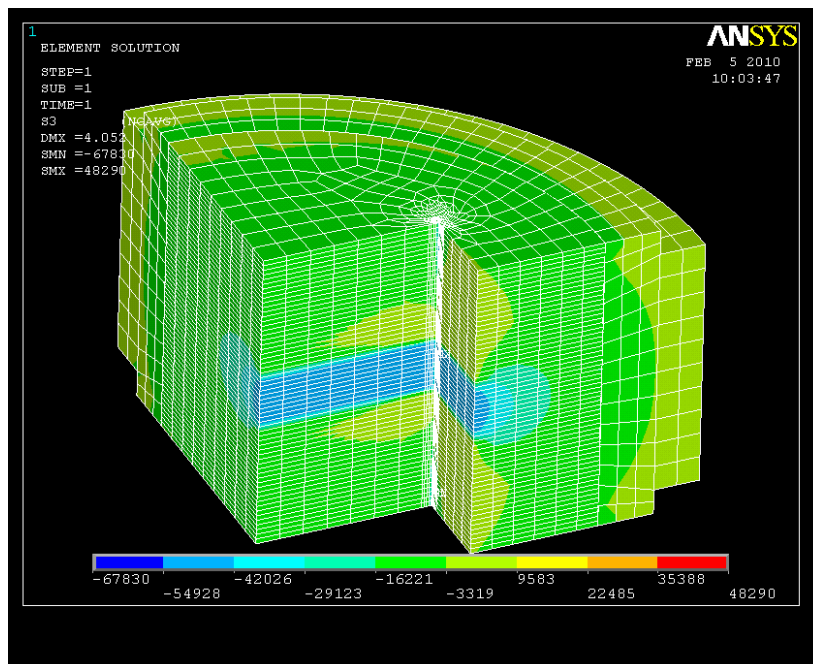


Fig. A.80. Third principal stress in europium oxide die with original geometry.

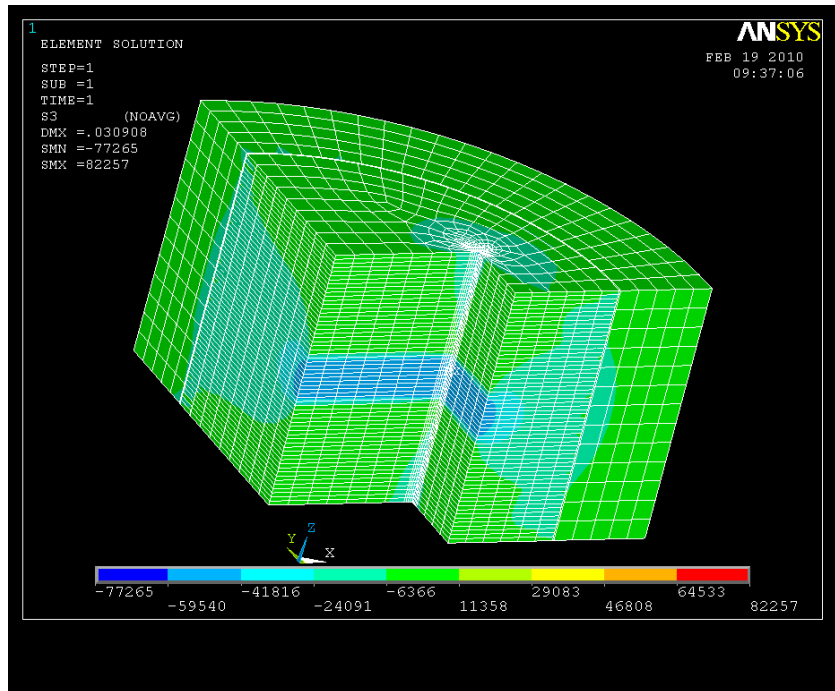


Fig. A.81. Third principal stress in europium oxide die with tantalum die's outer radius geometry.

INTERNAL DISTRIBUTION

1. Ethan Coffey
2. Brian Damiano
3. Daniel Pinkston
4. Charles Schaich
5. ORNL Office of Technical Information and Classification